Organic & Biomolecular Chemistry

PAPER

View Article Online
View Journal | View Issue

Cite this: *Org. Biomol. Chem.*, 2014, **12**, 316

Synthesis, structural characterization and reactivity of heteroazuliporphyrins†

Timothy D. Lash,* Jessica A. El-Beck and Gregory M. Ferrence

Received 3rd October 2013,
Accepted 12th November 2013

DOI: 10.1039/c3ob41992d

www.rsc.org/obc

A series of hetero-azuliporphyrins have been prepared by the "3 + 1" variant on the MacDonald condensation. Azulitripyrranes with *tert*-butyl and phenyl substituents reacted with thiophene or selenophene dialdehydes in the presence of TFA to give, following an oxidation step, thia- and selena-azuliporphyrins in 45–55% yield. Two of these compounds gave crystals suitable for X-ray crystallographic analysis and the data were consistent with the presence of a 17-atom delocalization pathway. The hetero-azuliporphyrins have significant diatropic character that is enhanced by the presence of an electron-donating *tert*-butyl substituent. The aromatic character is further increased in polar solvents such as DMSO, which are believed to stabilize dipolar resonance contributors with 18π electron delocalization pathways. Protonation also greatly increases the diatropic characteristics of these macrocycles. The porphyrinoids underwent an oxidative ring contraction with *t*-BuOOH–KOH to give moderate yields of benzoheterocarbaporphyrins. Reaction of azulitripyrranes with 2,5-furandicarbaldehyde afforded oxa-azuliporphyrins, a class of carbaporphyrinoids that had previously been inaccessible. These "missing links" in the study of heteroazuliporphyrins were isolated as the dihydrochloride salts. Protonated oxa-azuliporphyrins are stable aromatic compounds, but the free base forms underwent rapid decomposition in solution.

Introduction

Carbaporphyrinoid systems,[1–3] including N-confused porphyrins,[4] have been widely investigated over the last twenty years due to their intriguing spectroscopic and chemical properties. These systems differ from true porphyrins by having one of the internal nitrogen atoms substituted by a carbon, and depending on the specific structures may be fully aromatic, non-aromatic, or somewhere in between.[1] In addition to providing valuable insights into the aromatic characteristics of porphyrin-like systems,[5] carbaporphyrinoids have been shown to have unique reactivity and commonly undergo regioselective oxidation reactions.[1–4] Furthermore, carbaporphyrinoids readily form organometallic derivatives than can stabilize unusual oxidation states such as silver(III),[6] and these species show promise in the development of novel catalytic systems.[7] Azuliporphyrins (**1**) are an important family of carbaporphyrinoids where one of the pyrrolic units has been replaced with an azulene.[8] This system was originally prepared from a tripyrrane **2** and 1,3-azulenedicarbaldehyde **3** using a "3 + 1" variant on the MacDonald condensation (Scheme 1).[8,9] Subsequently, an alternative "3 + 1" strategy was developed where an azulitripyrrane **4** was condensed with a pyrrole dialdehyde **5** (Scheme 1).[10] In both approaches, an oxidation step is required to afford the fully conjugated porphyrinoid system. A "2 + 2" method for preparing an azuliporphyrin was also reported,[11] although much poorer yields were obtained, and a one-pot procedure for synthesizing tetraarylazuliporphyrins has also been described.[12] Azuliporphyrins show a significant degree of diatropic character, and the proton NMR spectra give an upfield resonance for the internal CH near 3 ppm.[13] This attribute has commonly been ascribed to dipolar resonance contributors such as **1′** that possess 18π electron delocalization pathways, as well as a fused tropylium unit.[8,9] These aromatic characteristics are enhanced in the protonated species, and the internal CH resonance shifts to approximately −3 ppm for solutions in TFA–$CDCl_3$.[8,9] Azuliporphyrins have been shown to be versatile organometallic ligands,[14,15] forming stable organometallic derivatives with nickel(II),[14] palladium(II),[14] platinum(II),[14] and iridium(III).[15] Furthermore, these porphyrinoids readily undergo oxidative ring contractions to form benzocarbaporphyrins,[16] and can be selectively oxidized at the internal carbon with copper(II) salts.[17] Benzo-fused azuliporphyrins have also been investigated and shown to possess extended conjugation pathways.[18] Due to these observations, related macrocyclic systems have been investigated such as heteroazuliporphyrins[9,10,19] and dicarbaporphyrinoid systems.[10,11,20] An azulitripyrrane **4** was obtained by reacting azulene with two

Department of Chemistry, Illinois State University, Normal, Illinois 61790-4160, USA. E-mail: tdlash@ilstu.edu

†Electronic supplementary information (ESI) available. CCDC 958530 and 958523. For ESI and crystallographic data in CIF or other electronic format see DOI: 10.1039/c3ob41992d

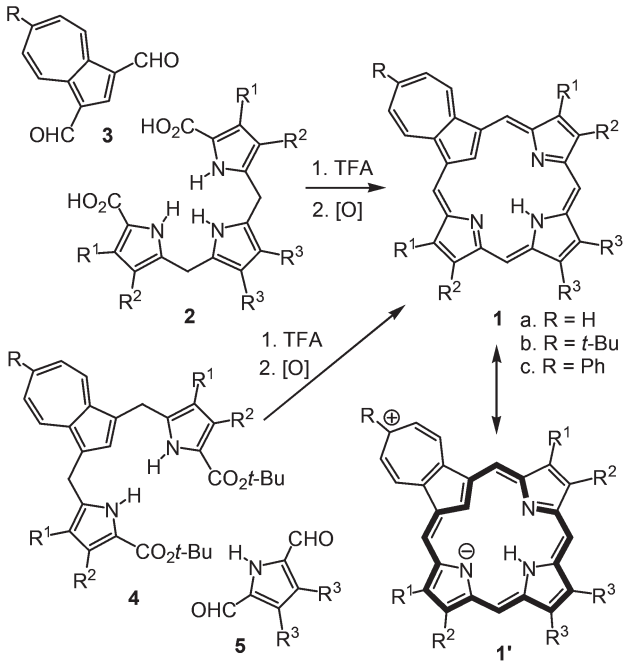

Scheme 1

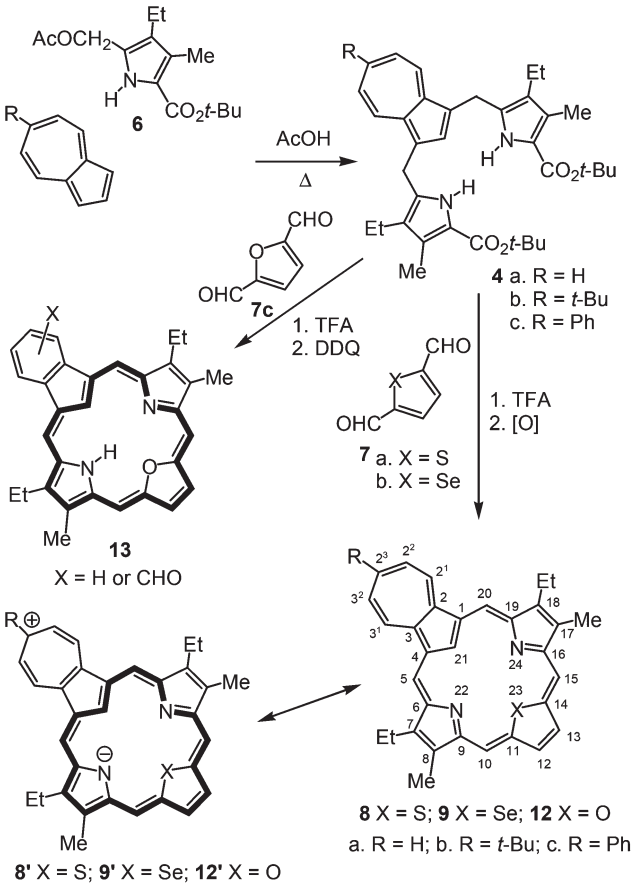

Scheme 2

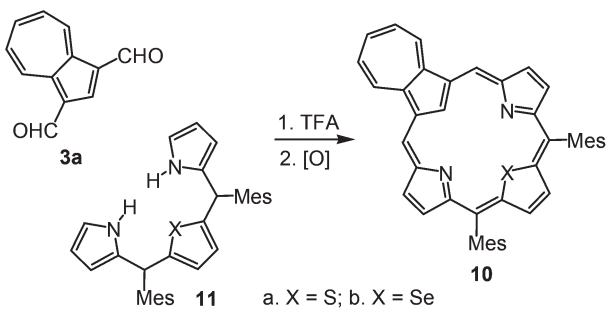

Scheme 3

equivalents of an acetoxymethylpyrrole **6** in refluxing acetic acid-isopropyl alcohol (Scheme 2).[10] The *tert*-butyl ester protective groups were cleaved with TFA, and subsequent reaction with 2,5-thiophenedicarbaldehyde (**7a**) and oxidation with DDQ gave a thia-azuliporphyrin **8a** in 33% yield.[10] Subsequently, selena-azuliporphyrin **9a** was prepared in a similar fashion (Scheme 2),[9] and dimesitylheteroazuliporphyrins **10** were obtained by reacting tripyrrane analogues **11** with azulene dialdehyde **3** (Scheme 3).[19] Thia- and selenaazuliporphyrins also have intermediary aromatic character and, like azuliporphyrins **1**, readily undergo oxidative ring contractions in the presence of *tert*-butyl hydroperoxide and potassium hydroxide to give heterobenzocarbaporphyrins.[9]

During the course of these studies, attempts were made to prepare oxa-azuliporphyrin **12a** by reacting azulitripyrrane **4a** with 2,5-furandicarbaldehyde (**7c**) in the presence of TFA in dichloromethane.[10] However, instead of the expected azuliporphyrin analogue, a series of benzo-oxacarbaporphyrins **13** were isolated instead (Scheme 2). The formation of these ring-contracted products is believed to have been triggered by a nucleophilic attack onto the seven-membered azulene ring, which is electron deficient due to incipient tropylium character.[16] In other studies, azuliporphyrins **4b** and **4c** with *tert*-butyl or phenyl substituents were prepared in order to increase the solubility of these porphyrinoid structures.[13,21] An added benefit of this study was that a *tert*-butyl substituted azuliporphyrin allowed the free base system to be structurally characterized for the first time by X-ray diffraction analysis.[13] We speculated that the presence of bulky substituents on the azulene ring might sterically inhibit the oxidative ring contractions and enable the isolation of oxa-azuliporphyrins, which represent a "missing link" in the study of heteroazuliporphyrin systems. Although the presence of a bulky substituent was later shown to be unnecessary, we set out to prepare a series of heteroazuliporphyrins with *tert*-butyl or phenyl substituents. It was anticipated that the *tert*-butyl and phenyl substituted porphyrinoids would have better solubility characteristics for spectroscopic analysis and could also facilitate the structural analysis of thia- and selena-azuliporphyrins. Hence, this approach potentially provides many benefits in the characterization of heteroazuliporphyrins. The results from these studies, including the isolation and characterization of the elusive oxa-azuliporphyrin system, are presented below.

Results and discussion

The synthesis of *tert*-butyl and phenyl substituted thia- and selena-azuliporphyrins was accomplished by reacting dialdehydes **7a** and **7b** with tripyrrane analogues **4b** and **4c** in TFA–CH_2Cl_2 (Scheme 2). The crude reaction mixtures were oxidized by shaking them with 0.1% aqueous ferric chloride solutions and, following purification by column chromatography and recrystallization from chloroform–hexanes, the porphyrinoids were isolated in 45–55% yield. These four hetero-azuliporphyrins gave green colored solutions and displayed typical azuliporphyrin-type UV-vis spectra[1] with multiple absorption bands between 350 and 500 nm, and a broad absorption at higher wavelengths (Fig. 1). Thiaazuliporphyrins **8b** and **8c** and selena-azuliporphyrin **9b** were reasonably soluble in chloroform and gave high quality proton and carbon-13 NMR spectra in $CDCl_3$. However, the solubility of phenylselena-azuliporphyrin **9c** was relatively poor and this prevented us from obtaining a high quality carbon-13 NMR spectrum for this structure. The proton NMR spectra for these porphyrinoids were insightful and confirmed the diatropic character of these ring systems. For instance, 2^3-*tert*-butylselena-azuliporphyrin **9b** showed a broad upfield resonance for the internal CH at 2.62 ppm, while the external *meso*-protons gave rise to two 2H singlets at relatively downfield values of 9.27 and 9.29 ppm (Fig. 2). The internal CH (21-H) for these structures did not show up in all of the spectra due to excessive broadening but could be identified for all four of the heteroazuliporphyrins. The shifts observed were compared to the values reported for the previously synthesized porphyrinoids **8a** and **9a**[9] and useful trends were observed (Table 1). The 21-H resonances for thia-azuliporphyrins **8** were slightly upfield from those observed for the corresponding selena-azuliporphyrins **9**, and the external 5,20-H values were shifted slightly further downfield. These data suggest that the diatropicity of thia-azuliporphyrins is slightly enhanced compared to the selena-macrocycles. However, the values for the 10,15-*meso*-protons appear to contradict this trend. The effects due to the azulene substituent were also assessed. The presence of a *tert*-butyl substituent in **8b** and **9b** causes the inner CH to shift upfield and the external *meso*-protons to move further downfield. A downfield shift can also be seen for the thiophene or selenophene protons (12,13-H). These results strongly imply that the diatropicity of the macrocycle is increased due to the presence of this electron-donating substituent, and this was attributed to stabilization of tropylium character in dipolar canonical forms such as **8′** and **9′**. The phenyl group exerts a far smaller effect, although the internal CH shifts slightly upfield compared to the 2^3-unsubstituted versions. This is to be expected as the phenyl moiety is a comparatively poor electron donor and steric factors will prevent significant conjugation effects. Significant solvent effects were also noted for these compounds. The chemical shifts for the *meso*-protons, the thiophene or selenophene protons, and the external azulene protons, were shifted downfield in acetone-d_6, and further downfield shifts were noted in DMSO-d_6. Unfortunately, the internal CH could not be identified in any of these spectra. These trends are illustrated for *tert*-butylthia-azuliporphyrin **8b** (Table 2). In acetone-d_6, downfield shifts of 0.16–0.38 ppm were noted for these resonances compared to $CDCl_3$, but the shifts in DMSO-d_6 were between 0.30 and 0.46 ppm. These data indicate that the dipolar character of

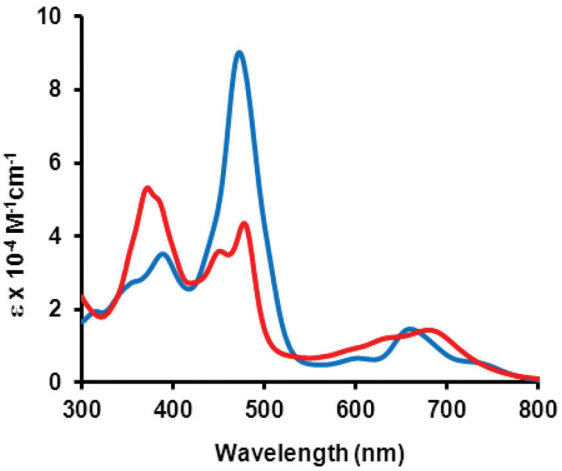

Fig. 1 UV-vis spectra of thia-azuliporphyrin **8b** in 1% Et_3N–$CHCl_3$ (red line) and 1% TFA–$CHCl_3$ (blue line).

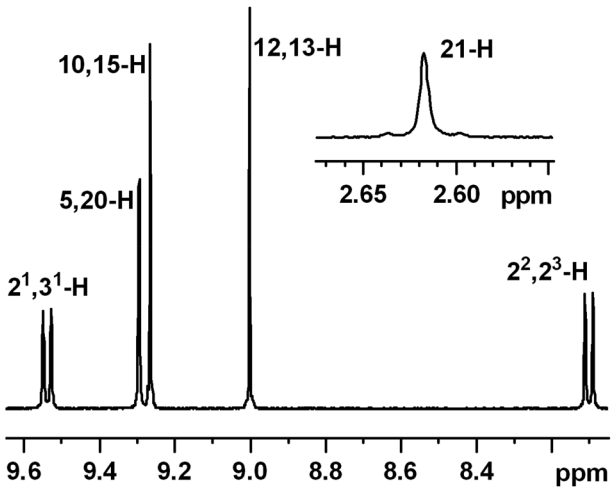

Fig. 2 Partial 500 MHz proton NMR spectrum of selena-azuliporphyrin **9b** in $CDCl_3$ showing the downfield region and the resonance for the internal CH.

Table 1 Selected chemical shifts for the proton NMR spectra of heteroazuliporphyrins **8** and **9** in $CDCl_3$. The data for **8a** and **9a** are taken from ref. 9

	21-H	12,13-H	10,15-H	5,20-H
8a	2.76	8.82	9.05	9.24
8b	2.33	8.88	9.14	9.33
8c	2.54	8.83	9.04	9.21
9a	3.04	8.93	9.18	9.21
9b	2.62	9.00	9.27	9.29
9c	2.91	8.94	9.18	9.18

Table 2 Selected chemical shifts for the proton NMR spectra of *tert*-butylthia-azuliporphyrin **8b** in different NMR solvents

NMR solvent	12,13-H	10,15-H	5,20-H	2^2,3^2-H	2^1,3^1-H
$CDCl_3$	8.88	9.14	9.33	8.11	9.56
Acetone-d_6	9.05	9.30	9.60	8.37	9.94
DMSO-d_6	9.18	9.44	9.67	8.41	10.10
Pyridine-d_5	9.17	9.52	9.84	8.01	9.87

these heteroazuliporphyrins is stabilized in polar solvents such as DMSO, and this enhances the diatropic properties of the system. Proton NMR spectra for **8b** and **9b** were also obtained in pyridine-d_5, but these results were more difficult to interpret. The 2^2,3^2-protons on the azulene ring were shifted upfield in this solvent, whereas the remaining external protons are shifted downfield to varying degrees (Table 2). These results may be due to the pyridine nitrogen interacting with the electron-deficient seven-membered ring. The proton and carbon-13 NMR spectra confirmed the presence of a plane of symmetry in these structures. For carbon-13 NMR spectra run in $CDCl_3$, the *meso*-carbons were observed between 111.3 and 113.3 ppm, while the internal carbon gave a resonance between 133.3 and 134.9 ppm.

Addition of TFA to solutions of **8** and **9** gave the corresponding dications $\mathbf{8}H_2^{2+}$ and $\mathbf{9}H_2^{2+}$ (Scheme 4). The UV-vis spectra of $\mathbf{8b}H_2^{2+}$, $\mathbf{8c}H_2^{2+}$, $\mathbf{9b}H_2^{2+}$ and $\mathbf{9c}H_2^{2+}$ in 1% TFA–$CHCl_3$ gave strong Soret-like bands at 472, 476, 503 and 508 nm, respectively, and two or three additional broad absorptions were noted between 580 and 800 nm (Fig. 1). The proton NMR spectra of $\mathbf{8}H_2^{2+}$ and $\mathbf{9}H_2^{2+}$ in TFA–$CDCl_3$ showed the expected enhanced diamagnetic ring currents, where the inner CH resonances shifted to between −2.6 and −4.0 ppm, while the *meso*-protons appeared downfield between 10.6 and 11.0 ppm (Fig. 3, Table 3). The 21-H resonances showed significantly larger upfield shifts for thiaazuliporphyrin dications $\mathbf{8}H_2^{2+}$ compared to the selenium versions $\mathbf{9}H_2^{2+}$, possibly indicating increased diatropicity in the thiophene structures. However, the resonances for the *meso*-protons did not show significant differences. The presence of a 2^3-*tert*-butyl substituent also led to an upfield shift for the 21-H resonance, although once again the external protons did not confirm this trend

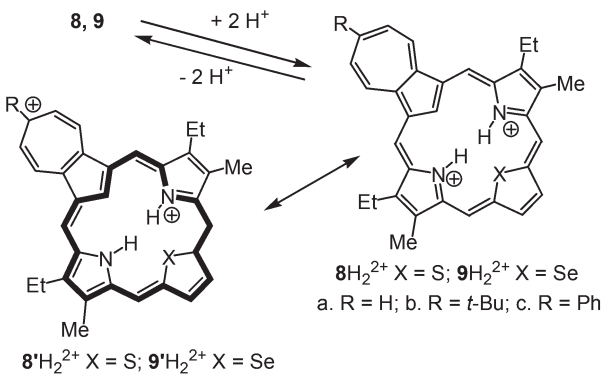

Scheme 4

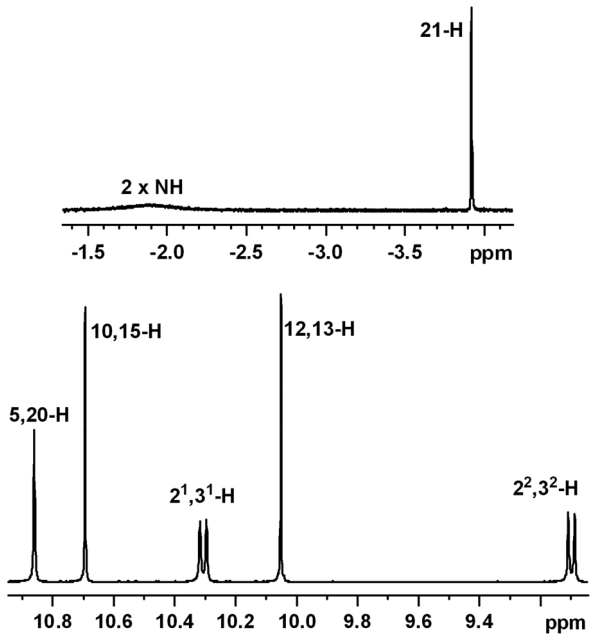

Fig. 3 Partial 500 MHz proton NMR spectrum of thia-azuliporphyrin dication $\mathbf{8b}H_2^{2+}$ in TFA–$CDCl_3$ showing the upfield and downfield regions.

Table 3 Selected chemical shifts for the proton NMR spectra of heteroazuliporphyrins dications **8** and **9** in TFA–$CDCl_3$. The data for $\mathbf{8a}H_2^{2+}$ and $\mathbf{9}H_2^{2+}$ are taken from ref. 9

	21-H	12,13-H	10,15-H	5,20-H
$\mathbf{8a}H_2^{2+}$	−3.44	9.99	10.60	10.86
$\mathbf{8b}H_2^{2+}$	−3.92	10.08	10.72	10.90
$\mathbf{8c}H_2^{2+}$	−3.86	10.12	10.78	10.94
$\mathbf{9a}H_2^{2+}$	−2.61	9.94	10.73	10.83
$\mathbf{9b}H_2^{2+}$	−2.83	9.91	10.71	10.81
$\mathbf{9c}H_2^{2+}$	−2.69	9.92	10.72	10.83

(Table 3). Nevertheless, the presence of a larger selenium unit would be expected to decrease the planarity of the dicationic species, thereby decreasing the diatropic ring current, while the *tert*-butyl group would be expected to have a beneficial effect in stabilizing resonance contributors such as $\mathbf{8a}'H_2^{2+}$ and $\mathbf{9a}'H_2^{2+}$ that possess 18π electron delocalization pathways.

The *tert*-butyl substituted heteroazuliporphyrins **8b** and **9b** both gave crystals that were suitable for X-ray diffraction analysis. The single crystal X-ray structure of **8b** confirmed the identity of the porphyrin analogue and demonstrated that the macrocycle is remarkably planar (Fig. 4). Difference Fourier maps clearly indicated the presence of electron density consistent with a hydrogen atom attached to the C(21) atom. The overall macrocycle is best classified as planar as evidence by the small 1.9(1)°, 8.81(6)°, 3.4(1)°, and 3.7(1)° tilts between the thiophene, azulene, and the two pyrrole planes and the mean macrocyclic plane defined by the *meso*, pyrrolic and C(1), C(2), C(3), and C(4) carbon atoms. A Mogul geometry check of **8b** indicated bonding parameters to be generally normal, with the N(22)–C(9)–C(10) and the N(24)–C(16)–C(15) angles being slightly acute. Not surprisingly, the C–S–C bond angle is a very

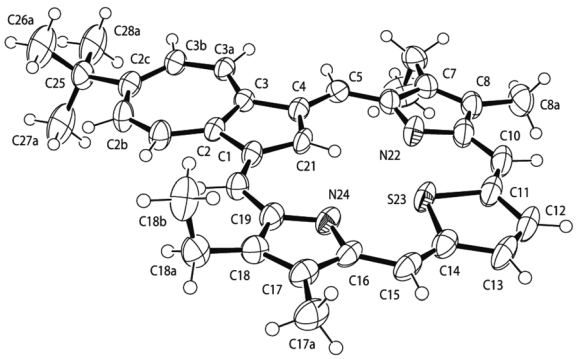

Fig. 4 ORTEP III drawing (50% probability level, hydrogen atoms drawn arbitrarily small) of thia-azuliporphyrin **8b**. Framework bond separations: C(1)–C(2) 1.448(6), C(2)–C(2a) 1.387(7), C(2a)–C(2b) 1.391(7), C(2b)–C(2c) 1.394(7), C(2c)–C(3b) 1.395(7), C(3b)–C(3a) 1.380(6), C(3a)–C(3) 1.379(6), C(2)–C(3) 1.446(7), C(3)–C(4) 1.449(6), C(4)–C(21) 1.395(7), C(21)–C(1) 1.404(7), C(4)–C(5) 1.416(7), C(5)–C(6) 1.383(7), C(6)–C(7) 1.460(7), C(7)–C(8) 1.353(7), C(8)–C(9) 1.460(8), C(9)–C(10) 1.415(8), C(10)–C(11) 1.373(8), C(11)–C(12) 1.425(8), C(12)–C(13) 1.352(9), C(13)–C(14) 1.439(8), C(14)–C(15) 1.362(8), C(15)–C(16) 1.419(7), C(16)–C(17) 1.456(7), C(17)–C(18) 1.353(7), C(18)–C(19) 1.469(7), C(19)–C(20) 1.385 (6), C(20)–C(1) 1.411(7), C(6)–N(22) 1.380(7), N(22)–C(9) 1.330(7), C(11)–S(23) 1.753(6), S(23)–C(14) 1.752(6), C(16)–N(24) 1.341(6), N(24)–C(19) 1.371(6) Å.

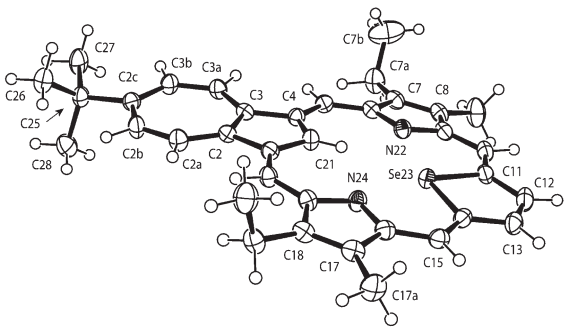

Fig. 5 ORTEP III drawing (50% probability level, hydrogen atoms drawn arbitrarily small) of selena-azuliporphyrin **9b**. Framework bond separations: C(1)–C(2) 1.447(4), C(2)–C(2a) 1.384(4), C(2a)–C(2b) 1.389(4), C(2b)–C(2c) 1.395(4), C(2c)–C(3b) 1.396(4), C(3b)–C(3a) 1.394(4), C(3a)–C(3) 1.382(4), C(2)–C(3) 1.449(4), C(3)–C(4) 1.448(4), C(4)–C(21) 1.400 (4), C(21)–C(1) 1.402(4), C(4)–C(5) 1.424(4), C(5)–C(6) 1.382(4), C(6)–C(7) 1.465(4), C(7)–C(8) 1.358(4), C(8)–C(9) 1.453(4), C(9)–C(10) 1.422 (4), C(10)–C(11) 1.372(4), C(11)–C(12) 1.426(4), C(12)–C(13) 1.359(5), C(13)–C(14) 1.429(4), C(14)–C(15) 1.366(4), C(15)–C(16) 1.424(4), C(16)–C(17) 1.456(4), C(17)–C(18) 1.353(4), C(18)–C(19) 1.469(4), C(19)–C(20) 1.376(4), C(20)–C(1) 1.429(4), C(6)–N(22) 1.376(4), N(22)–C(9) 1.343(4), C(11)–Se(23) 1.890(3), Se(23)–C(14) 1.892(3), C(16)–N(24) 1.341(4), N(24)–C(19) 1.377(4) Å.

acute 92.3(3)°, consistent with sp^2 hybridization of the sulfur. The same type of analysis was also performed on selena-azuliporphyrin **9b**, which was also shown to be surprisingly flat (Fig. 5). The overall macrocycle is again best classified as planar as evidenced by the small 2.70(5)°, 6.95(4)°, 7.14(8)°, and 3.49(8)° tilts between the selenophene, azulene, and two pyrrole planes and the mean macrocyclic plane defined by the *meso*, pyrrolic and C(1), C(2), C(3) and C(4) carbon atoms. The Mogul geometry check for **9b** also indicated bonding parameters to be generally normal with the N(22)–C(9)–C(10) and the N(24)–C(16)–C(15) angles being slightly acute, and the C–Se–C bond angle is a very acute 87.8(1)°.

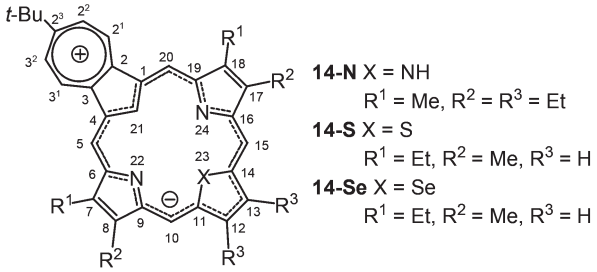

The X-ray crystal structure of *tert*-butylazuliporphyrin **1b** had previously been shown to have bond lengths that were consistent with a species that has a significant degree of character derived from canonical forms with a 17-atom delocalization pathway, as illustrated for hybrid structure **14-N**.[13] This bonding arrangement is supported by Aihara's graph theory analysis,[22] and to a lesser extent by density functional theory calculations for azuliporphyrin.[23] An analysis of the bond lengths for heteroazuliporphyrins **8b** and **9b** are also consistent with contributions from similar species, *i.e.* hybrid structures **14-S** and **14-Se**. For thia-azuliporphyrin **8b**, the C–C bonds within this pathway fall into a range of 1.352(9)–1.439(8) Å, apart from two anomalous bond lengths within the thiophene ring, values that are intermediary between single and double bonds. In addition, the C1–C2, C3–C4, C6–C7, C8–C9, C16–C17 and C18–C19 C–C bonds, which are connected to but outside of the pathway, have values between 1.448(6) and 1.395(7) Å, bond lengths that are closer to being single bond-like. The C7–C8 and C17–C18 bond lengths are both 1.353(7) Å, a value that is much more double bond-like as predicted by this model. Furthermore, six of the C–C bonds in the seven-membered ring fall into the range of 1.379(6)–1.446(7) Å, values that are consistent with a structural unit that has tropylium character. However, the C2–C3 bond is relatively long (1.446(7) Å) and, as has already been noted, the bond lengths in the thiophene ring are outliers. Although the analysis is not unequivocal, the bond lengths do point to the 17-atom delocalization pathway in **14-S** being at least partially responsible for the aromatic characteristics for this compound. In fact, all framework bond lengths of **8b** are indistinguishable from those observed in the closely related 10,15-dimesityl-23-thia-azuliporphyrin.[19] An analysis of the bond lengths for **9b** shows the same trends and implies that **14-Se** is also a significant contributor for the selena-azuliporphyrin system.

Heteroazuliporphyrins **8b**, **8c**, **9b** and **9c** were reacted with *t*-BuOOH–KOH in a mixture of dichloromethane and methanol, and afforded moderate yields of the corresponding benzoheterocarbaporphyrins **15** and **16** (Scheme 5). The 2^2-substituted structures **15** were the major products in each case and were isolated in 34–43%, but a minor aldehydic product **16** was noted in each case. The minor product proved to be very difficult to isolate, but samples of the phenyl

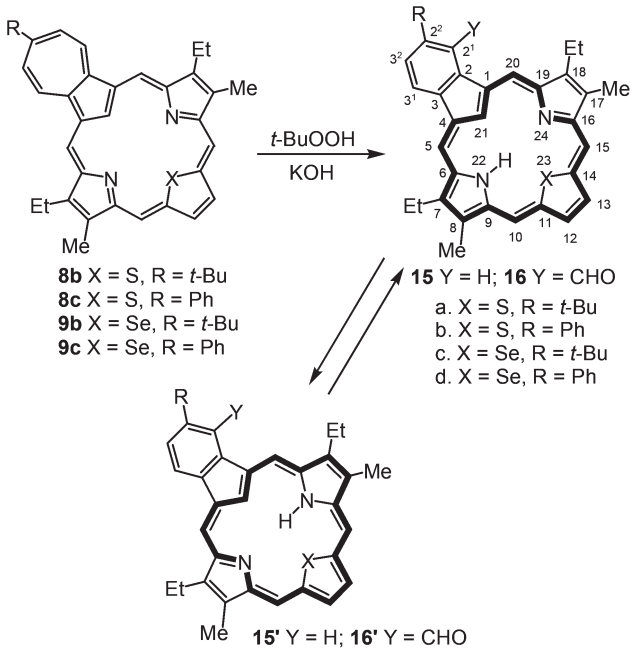

Scheme 5

substituted versions **16b** and **16d** were obtained in 90–95% purity. The structures were assigned on the basis of proton, carbon-13, COSY, HSQC and nOe difference proton NMR spectroscopy, and high resolution mass spectrometry. This type of ring contraction is believed to involve an initial nucleophilic attack by the *tert*-butyl peroxide anion onto the electron-deficient seven-membered ring (Scheme 6).[16] Subsequent Cope rearrangement would then give the norcaradiene derivatives **17** (Scheme 6).[24] Elimination of *tert*-butyl alcohol could afford the fused cyclopropanone intermediates **18**, and following a cheleotropic elimination of carbon monoxide, the observed 2^2-substituted benzoheterocarbaporphyrins **15** would be formed. Alternatively, abstraction of a bridgehead proton from **17** with loss of *tert*-butoxide would directly lead to the minor aldehyde products **16** (Scheme 6). The proton NMR spectra for the heterocarbaporphyrins demonstrated that these structures are aromatic compounds that exhibit large diamagnetic ring currents. For instance, **15a** gave upfield resonances at −5.47 and −4.41 ppm for the 21-H and NH, respectively, while the external *meso*-protons gave rise to four downfield singlets at 10.12, 10.16, 10.300 and 10.304 ppm. The carbon-13 NMR spectra for **15** and **16** in $CDCl_3$ were of a poor quality, in part due to the low solubility of these compounds. The expected number of carbon resonances could not be identified and broad peaks were also observed. These results were attributed to the heterocarbaporphyrins existing as two slightly different tautomers (Scheme 5) that interconvert at a moderate rate on the carbon-13 NMR time scale. This would be expected to lead to broadening of the carbon resonances, particularly for the α-selenophene and pyrrole carbons. The poor solubility of these samples made further investigations into this phenomenon impractical.

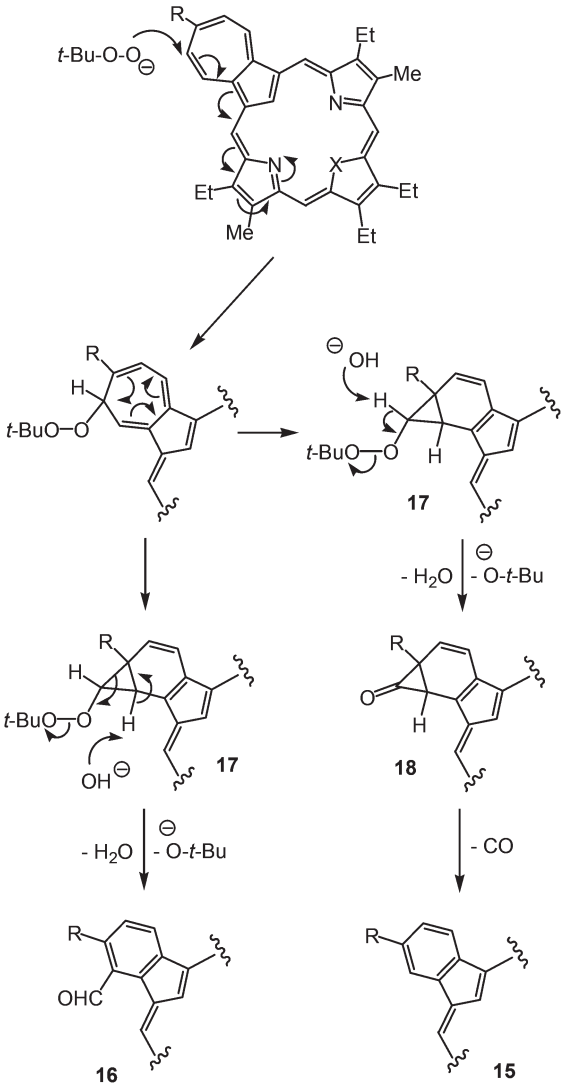

Scheme 6

Following on from these studies, the preparation of oxa-azuliporphyrins was attempted (Scheme 7). Initially, when azulitripyrrane **4b** was reacted with furan dialdehyde **7c** in the presence of TFA, and then oxidized with DDQ or ferric chloride, no identifiable products could be isolated. However, when the crude reaction solution was oxidized by shaking it with an aqueous solution of ferric chloride, and then washed with a saturated sodium chloride solution, a heavy precipitate was generated. This precipitate was totally insoluble in chloroform, but dissolved in methanol to give bright green colored solutions. The product was purified by column chromatography on silica, eluting with 15% methanol–chloroform, and the product fraction was then treated with a solution of HCl in ether to ensure that the sample was completely protonated. Following recrystallization, the oxa-azuliporphyrin **12b** was isolated as the dihydrochloride salt in 57% yield. The reaction was also successful with phenyl-substituted azulitripyrrane **4c** and the related oxa-azuliporphyrin dihydrochloride salt **12c**·2HCl was isolated in 41% yield. It was quickly established

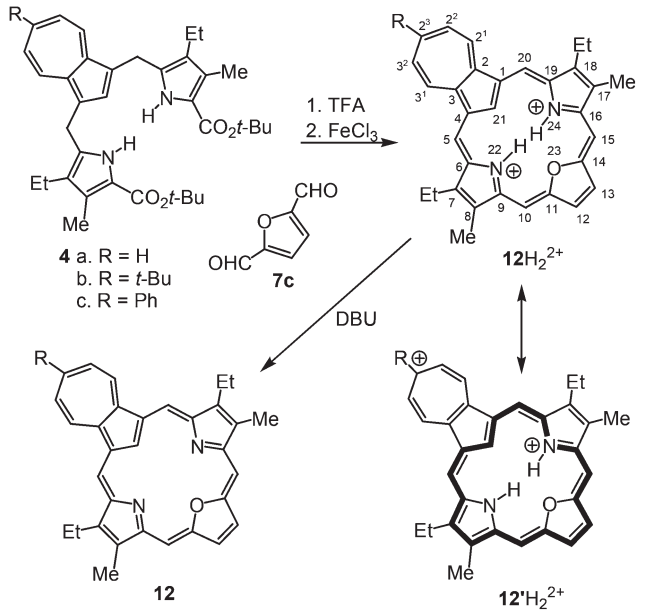

Scheme 7

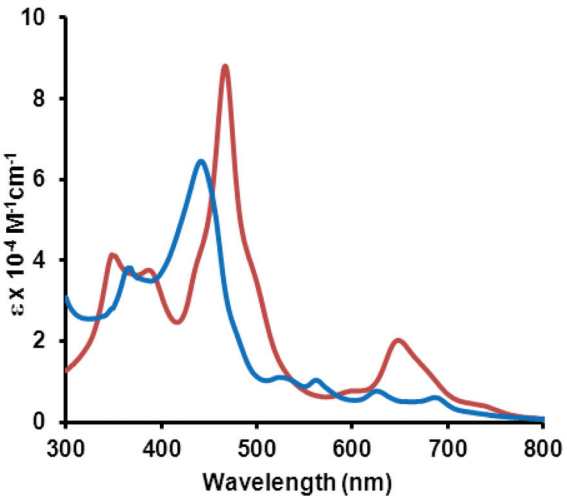

Fig. 6 UV-vis spectra of oxa-azuliporphyrin **12a**·2HCl in chloroform (red line) and 2% DBU–$CHCl_3$ (blue line).

that the presence of a substituent on the azulene moiety had nothing to do with the success of this chemistry, as equally good results were obtained with **4a**. Hence, when **4a** was reacted with **7c** under the same conditions, **12a**·2HCl was isolated in 53% yield. The UV-vis spectrum of the dihydrochloride salts showed the presence of a strong Soret-like band between 460 and 470 nm, and several broad absorptions at longer wavelengths (Fig. 6). In this respect, the data for the protonated oxa-azuliporphyrins $\mathbf{12}H_2^{2+}$ resembled the results for **8** and **9**. The generation of the free base forms for the oxa-azuliporphyrins was problematical due to the instability of these species. However, spectra could be obtained in 2% DBU–chloroform and these showed a diminished Soret band and a series of Q-type absorptions (Fig. 6). Addition of TFA to solutions of **12**·2HCl in chloroform induced minor changes in the spectra, including a slight intensification of the Soret band, but this was attributed to hydrogen bonding interactions. The poor solubility of the hydrochloride salts made it difficult to obtain NMR data. However, the samples were sufficiently soluble in methanol-d_4 to obtain proton and carbon-13 NMR spectra. Some of the proton NMR signals were broadened, presumably due to aggregation effects. The ^{1}H NMR spectra for **12**·2HCl showed substantial diamagnetic ring currents and the internal 21-H was observed near −3.5 ppm. The *meso*-protons were also considerably shifted downfield to between 10.3 and 11.1 ppm, while the furan protons appeared near 10 ppm. These chemical shift values indicate that dications $\mathbf{12}H_2^{2+}$ have comparable diatropic character to those seen for thia- and selena-azuliporphyrin dications $\mathbf{8}H_2^{2+}$ and $\mathbf{9}H_2^{2+}$. Although the samples were completely insoluble in $CDCl_3$, NMR data could be obtained in TFA–$CDCl_3$ and these results showed the same trends, although the upfield shifts for the 21-H resonance and the downfield shifts for the *meso*-proton resonances were slightly reduced. For instance, $\mathbf{12a}H_2^{2+}$ in TFA–$CDCl_3$ showed the 21-H resonance at −3.21 ppm, while the *meso*-protons gave rise to two 2H singlets at 9.90 and 10.66 ppm. Proton NMR spectra for **12a** and **12b** were obtained in DBU–$CDCl_3$, although only the downfield region could be observed. The *meso*-protons for **12a** appeared at 8.35 and 8.90 ppm, values that are slightly upfield from the corresponding resonances for thia- and selena-azuliporphyrins **8** and **9**. In the carbon-13 NMR spectra for **12a–c**·2HCl in methanol-d_4 or TFA–$CDCl_3$, the interior carbon was observed between 125.4 and 126.5 ppm, while the *meso*-carbons appeared near 97 ppm (10,15-C) and 113 ppm (C-5,20). The proton and carbon-13 NMR spectra also confirmed that the structures possess a plane of symmetry. Reaction of oxa-azuliporphyrins **12** with *t*-BuOOH and KOH afforded complex mixtures and ring contraction products could not be isolated. This is most likely due to the instability of the free base species.

Conclusion

A series of heteroazuliporphyrins were prepared with 2^3-*tert*-butyl and 2^3-phenyl substituents using a "3 + 1" strategy. Thia- and selena-azuliporphyrins were formed in excellent yields and showed significant diatropic characteristics that were enhanced in the protonated species. The presence of a *tert*-butyl group on the azulene unit slightly increased the diatropic properties of these porphyrinoid macrocycles, and significant changes were also noted in polar solvents. Two of the heteroazuliporphyrins gave crystals suitable for X-ray crystallographic analysis, and the macrocycles were shown to be essentially planar with bond lengths that were consistent with the presence of a favored 17-atom delocalization pathway. Oxidative ring contractions of thia- and selena-azuliporphyrins were observed in the presence of *t*-BuOOH and KOH to give benzoheterocarbaporphyrins, and the presence of 2^3-*tert*-butyl or

phenyl substituents did not inhibit these reactions. Reactions of azulitripyrranes with 2,5-furandicarbaldehyde afforded oxa-azuliporphyrins, a missing link in the study of azuliporphyrin systems, and these were isolated as the aromatic dihydrochloride salts. Although the protonated species were stable, the free base forms rapidly underwent decomposition. Overall, these studies have significantly extended our understanding of azuliporphyrin-type systems and have allowed the characterization of hitherto unknown oxa-azuliporphyrins.

Experimental

Melting points are uncorrected. UV-vis data are reported as λ_{max}/nm (log [ε/M^{-1} cm^{-1}]). NMR spectra were recorded using a 400 or 500 MHz NMR spectrometer. Chemical shifts are reported in parts per million (ppm) relative to $CDCl_3$ (^{1}H residual $CHCl_3$ δ 7.26, ^{13}C $CDCl_3$ triplet δ 77.23), methanol-d_4 (^{1}H residual CHD_2OD quintet δ 3.30, ^{13}C CD_3OD septet δ 49.0), acetone-d_6 (^{1}H acetone-d_5 residual quintet δ 2.04), DMSO-d_6 (^{1}H DMSO-d_5 residual quintet δ 2.49) or pyridine-d_5 (^{1}H pyridine-d_4 residual peak at δ 7.19). ^{1}H NMR values are reported as chemical shifts δ, relative integral, multiplicity (s, singlet; d, doublet; t, triplet; q, quartet; m, multiplet; br, broad peak) and coupling constant (J). Coupling constants were taken directly from the spectra. 2D experiments were performed by using standard software. High-resolution mass spectrometry (HRMS) was carried out by either electron impact (EI+) or electrospray ionization (ESI) on a MicroTOF-Q mass spectrometer. ^{1}H and ^{13}C NMR spectra for all new compounds are reported in ESI.†

2^3-*tert*-Butyl-7,18-tetraethyl-8,17-dimethyl-23-thiaazuliporphyrin (8b)

Azulitripyrrane analogue **4b** (110 mg, 0.176 mmol) was stirred in TFA (3 mL) under nitrogen for 10 min. The reaction mixture was diluted with dichloromethane (100 mL), 2,5-thiophenedicarbaldehyde (41 mg, 0.29 mmol) was added, and the solution stirred overnight in the dark. The solution was shaken vigorously in a separatory funnel with 0.1% aqueous ferric chloride solution (150 mL) for 5 min. The organic layer was separated and the aqueous solution back extracted with chloroform. The combined organic solutions were washed with water and then with a 5% aqueous sodium bicarbonate solution, and the organic phase was dried over sodium sulfate and evaporated under reduced pressure. The residue was purified on a grade 3 basic alumina column, eluting with chloroform, and the product was collected as a deep green fraction that followed a brown prefraction. The solvent was removed on a rotary evaporator and the residue recrystallized from chloroform–hexanes to give the *tert*-butylazuliporphyrin (43.6 mg, 0.0826 mmol, 47%) as dark purple crystals. Mp: >300 °C. UV-vis (1% Et_3N–$CHCl_3$): λ_{max} (log ε) 372 (4.73), 383 (sh, 4.70), 451 (4.55), 478 (4.64), 634 (sh, 4.08), 680 (4.16). UV-vis (1% TFA–$CHCl_3$): λ_{max} (log ε) 350 (sh, 4.43), 389 (4.54), 472 (4.95), 602 (sh, 3.83), 660 (4.17), 733 (sh, 3.75). ^{1}H NMR (500 MHz, $CDCl_3$): δ 1.63 (6H, t, J = 7.7 Hz, 2 × CH_2CH_3), 1.65 (9H, s, *t*-Bu), 2.33 (1H, br s, 21-H), 2.92 (6H, s, 8,17-CH_3), 3.48 (4H, q, J = 7.7 Hz, 7,18-CH_2), 8.11 (2H, d, J = 10.7 Hz, 2^2,3^2-H), 8.88 (2H, s, 12,13-H), 9.14 (2H, s, 10,15-H), 9.33 (2H, s, 5,20-H), 9.56 (2H, d, J = 10.7 Hz, 2^1,3^1-H). ^{1}H NMR (400 MHz, acetone-d_6): δ 1.63 (6H, t, J = 7.6 Hz), 1.70 (9H, s), 2.94 (6H, s), 3.56 (4H, q, J = 7.6 Hz), 8.37 (2H, d, J = 11.2 Hz), 9.05 (2H, s), 9.30 (2H, s), 9.60 (2H, s), 9.94 (2H, d, J = 11.2 Hz). ^{1}H NMR (400 MHz, DMSO-d_6): δ 1.60 (6H, t, J = 7.7 Hz), 1.65 (9H, s), 2.94 (6H, s), 3.56 (4H, q, J = 7.7 Hz), 8.41 (2H, d, J = 11.2 Hz), 9.18 (2H, s), 9.44 (2H, s), 9.67 (2H, s), 10.10 (2H, d, J = 11.2 Hz). ^{1}H NMR (400 MHz, pyridine-d_5): δ 1.51 (9H, s), 1.65 (6H, t, J = 7.6 Hz), 2.91 (6H, s), 3.57 (4H, q, J = 7.6 Hz), 8.01 (2H, d, J = 11.2 Hz), 9.17 (2H, s), 9.52 (2H, s), 9.78 (2H, d, J = 11.2 Hz), 9.84 (2H, s). ^{1}H NMR (500 MHz, TFA–$CDCl_3$): δ −3.92 (1H, s, 21-H), −1.89 (2H, br s, 2 × NH), 1.78 (9H, s, *t*-Bu), 1.79 (6H, t, J = 7.8 Hz, 2 × CH_2CH_3), 3.52 (6H, s, 8,17-CH_3), 4.07 (4H, q, J = 7.8 Hz, 7,18-CH_2), 9.11 (2H, d, J = 10.7 Hz, 2^2,3^2-H), 10.08 (2H, s, 12,13-H), 10.33 (2H, d, J = 10.7 Hz, 2^1,3^1-H), 10.72 (2H, s, 10,15-H), 10.90 (2H, s, 5,20-H). ^{13}C NMR ($CDCl_3$): δ 10.8 (8,17-CH_3), 17.4 (2 × CH_2CH_3), 19.5 (7,18-CH_2), 32.0 (C(CH_3)$_3$), 39.2 (C(CH_3)$_3$), 111.3 (5,20-C), 111.8 (10,15-C), 126.9, 131.3 (2^2,3^2-C), 134.5, 134.6 (2^1,3^1-C), 134.94 (21-C), 135.01 (12,13-C), 147.2, 150.0, 151.3, 152.5, 162.6, 165.2. ^{13}C NMR (TFA–$CDCl_3$): δ 11.4 (8,17-CH_3), 16.6 (2 × CH_2CH_3), 20.3 (7,18-CH_2), 31.5 (C(CH_3)$_3$), 41.2 (C(CH_3)$_3$), 111.49 (5,20-C), 111.55 (10,15-C), 121.7 (21-C), 131.0, 138.5, 139.5 (12,13-C), 140.7 2^1,3^1-C), 141.0, 143.8 (2^2,3^2-C), 147.8, 149.2, 149.7, 156.0, 176.8. HRMS (ESI) m/z: calcd for $C_{36}H_{36}N_2S$ + H, 529.2677; found, 529.2684. Anal. calcd for $C_{36}H_{36}N_2S$·1/3$CHCl_3$: C, 76.76; H, 6.44; N, 4.93. Found: C, 76.79; H, 6.49; N, 4.91.

7,18-Diethyl-8,17-dimethyl-2^3-phenyl-23-thiaazuliporphyrin (8c)

Using the same procedure, tripyrrane analogue **4c** (114 mg, 0.176 mmol) gave the thiaazuliporphyrin (43.3 mg, 0.079 mmol, 45%) as dark green crystals (chloroform–hexanes). Mp: >300 °C. UV-vis (1% Et_3N–$CHCl_3$): λ_{max} (log ε) 374 (4.77), 385 (sh, 4.75), 451 (4.63), 479 (4.72), 622 (sh, 4.18), 675 (4.20). UV-vis (1% TFA–$CHCl_3$): λ_{max} (log ε) 356 (4.56), 397 (4.61), 476 (5.02), 606 (sh, 3.93), 662 (4.25), 746 (sh, 3.78). ^{1}H NMR (500 MHz, $CDCl_3$): δ 1.60 (6H, t, J = 7.6 Hz, 2 × CH_2CH_3), 2.54 (1H, br s, 21-H), 2.88 (6H, s, 8,17-CH_3), 3.45 (4H, q, J = 7.7 Hz, 7,18-CH_2), 7.58 (1H, t, J = 7.3 Hz, *p*-H), 7.63 (2H, t, J = 7.3 Hz, *m*-H), 7.82 (2H, d, J = 7.3 Hz, *o*-H), 8.06 (2H, d, J = 10.2 Hz, 2^2,3^2-H), 8.83 (2H, s, 12,13-H), 9.04 (2H, s, 10,15-H), 9.21 (2H, s, 5,20-H), 9.52 (2H, d, J = 10.2 Hz, 2^1,3^1-H). ^{1}H NMR (500 MHz, acetone-d_6): δ 1.59 (6H, t, J = 7.7 Hz), 2.91 (6H, s), 3.51 (4H, q, J = 7.7 Hz), 7.64 (1H, t, J = 7.4 Hz), 7.71 (2H, t, J = 7.5 Hz), 8.02 (2H, d, J = 7.5 Hz), 8.30 (2H, d, J = 10.4 Hz), 9.02 (2H, s), 9.23 (2H, s), 9.44 (2H, s), 9.90 (2H, d, J = 10.4 Hz). ^{1}H NMR (500 MHz, DMSO-d_6): δ 1.59 (6H, t, J = 7.6 Hz), 2.92 (6H, s), 3.56 (4H, q, J = 7.6 Hz), 7.65 (1H, t, J = 7.4 Hz), 7.72 (2H, t, J = 7.5 Hz), 8.03 (2H, d, J = 7.7 Hz), 8.38 (2H, d, J = 10.5 Hz), 9.15 (2H, s), 9.39 (2H, s), 9.65 (2H, s), 10.14 (2H, d, J = 10.4 Hz). ^{1}H NMR (500 MHz, TFA–$CDCl_3$): δ −3.86 (1H, s,

21-H), −2.20 (2H, br s, 2 × NH), 1.80 (6H, t, J = 7.7 Hz, 2 × CH_2CH_3), 3.55 (6H, s, 8,17-CH_3), 4.11 (4H, q, J = 7.7 Hz, 7,18-CH_2), 7.77–7.80 (3H, m, *m*- & *p*-H), 7.97–8.00 (2H, m, *o*-H), 9.14 (2H, d, J = 10.6 Hz, 2^2,3^2-H) 10.12 (2H, s, 12,13-H), 10.41 (2H, d, J = 10.6 Hz, 2^1,3^1-H), 10.78 (2H, s, 10,15-H), 10.94 (2H, s, 5,20-H). ^{13}C NMR ($CDCl_3$): δ 10.8 (8,17-CH_3), 17.4 (2 × CH_2CH_3), 19.4 (7,18-CH_2), 111.3 (5,20-C), 111.7 (10,15-C), 127.2, 128.5 (*o*-C), 129.46, 129.54 (*m*- & *p*-C), 133.5 (2^2,3^2-C), 134.6, 135.0 (12,13-C), 135.1 (2^1,3^1-C), 147.3. ^{13}C NMR (TFA–$CDCl_3$): δ 11.5 (8,17-CH_3), 16.6 (2 × CH_2CH_3), 20.2 (7,18-CH_2), 111.4 (10,15-C, 112.0 (5,20-C), 122.1 (21-C), 129.3 (*p*-C), 130.5 (*o*-C), 130.9, 132.2 (*p*-C), 138.0, 139.4 (12,13-C), 140.6 (2^1,3^1-C), 141.1, 144.6 (2^2,3^2-C), 148.3, 149.5, 149.7, 155.2, 163.1. HRMS (ESI) m/z: calcd for $C_{38}H_{32}N_2S$ + H, 549.2364; found, 549.2381. Anal. calcd for $C_{38}H_{32}N_2S$·1/8$CHCl_3$: C, 81.24; H, 5.74; N, 4.97. Found: C, 80.94; H, 5.72; N, 4.95.

2^3-*tert*-Butyl-7,18-tetraethyl-8,17-dimethyl-23-selenaazuliporphyrin (9b)

Using the same procedure, tripyrrane analogue **4b** (110 mg, 0.176 mmol) and 2,5-selenophenedicarbaldehyde (55 mg, 0.29 mmol) gave the selenaazuliporphyrin (56.2 mg, 0.0976 mmol, 55%) as dark green crystals (chloroform–hexanes). Mp: >300 °C. UV-vis (1% Et_3N–$CHCl_3$): λ_{max} (log ε) 363 (4.75), 400 (4.67), 450 (4.65), 477 (4.70) 587 (sh, 4.07), 628 (sh, 4.18), 675 (4.24). UV-vis (1% TFA–$CHCl_3$): λ_{max} (log ε) 368 (4.60), 392 (sh, 4.52), 503 (4.94), 667 (4.14), 754 (sh, 3.72). ^{1}H NMR (500 MHz, $CDCl_3$): δ 1.62 (6H, t, J = 7.7 Hz, 2 × CH_2CH_3), 1.64 (9H, s, *t*-Bu), 2.62 (1H, s, 21-H), 2.89 (6H, s, 8,17-CH_3), 3.46 (4H, q, J = 7.7 Hz, 7,18-CH_2), 8.10 (2H, d, J = 10.8 Hz, 2^2,3^2-H), 9.00 (2H, s, 12,13-H), 9.27 (2H, s, 10,15-H), 9.29 (2H, s, 5,20-H), 9.54 (2H, d, J = 10.8 Hz, 2^1,3^1-H). ^{1}H NMR (400 MHz, acetone-d_6, downfield region only): δ 8.38 (2H, d, J = 10.8 Hz), 9.14 (2H, s), 9.42 (2H, s), 9.60 (2H, s), 9.96 (2H, d, J = 10.8 Hz). ^{1}H NMR (400 MHz, DMSO-d_6): δ 1.57 (6H, t, J = 7.7 Hz), 1.64 (9H, s), 2.90 (6H, s), 3.54 (4H, q, J = 7.7 Hz), 8.41 (2H, d, J = 11.2 Hz), 9.25 (2H, s), 9.53 (2H, s), 9.65 (2H, s), 10.09 (2H, d, J = 11.2 Hz). ^{1}H NMR (400 MHz, pyridine-d_5): δ 1.51 (9H, s), 1.63 (6H, t, J = 7.6 Hz), 2.89 (6H, s), 3.54 (4H, q, J = 7.6 Hz), 8.02 (2H, d, J = 10.8 Hz), 9.32 (2H, s), 9.63 (2H, s), 9.78 (2H, d, J = 10.8 Hz), 9.81 (2H, s). ^{1}H NMR (500 MHz, TFA–$CDCl_3$): δ −2.83 (1H, s, 21-H), −1.59 (2H, br s, 2 × NH), 1.76 (9H, s, *t*-Bu), 1.79 (6H, t, J = 7.7 Hz, 2 × CH_2CH_3), 3.49 (6H, s, 8,17-CH_3), 4.06 (4H, q, J = 7.7 Hz, 7,18-CH_2), 9.08 (2H, d, J = 10.6 Hz, 2^2,3^2-H), 9.91 (2H, s, 12,13-H), 10.27 (2H, d, J = 10.6 Hz, 2^1,3^1-H), 10.71 (2H, s, 10,15-H), 10.81 (2H, s, 5,20-H). ^{13}C NMR ($CDCl_3$): δ 10.8 (8,17-CH_3), 17.4 (2 × CH_2CH_3), 19.5 (7,18-CH_2), 32.0 ($C(CH_3)_3$), 39.2 ($C(CH_3)_3$), 111.9 (5,20-C), 115.2 (10,15-C), 126.1, 130.9 (2^2,3^2-C), 133.3 (21-C), 134.3, 134.5 (2^1,3^1-C), 137.1 (12,13-C), 147.4, 149.1, 151.4, 155.8, 164.1, 165.2. ^{13}C NMR (TFA–$CDCl_3$): δ 11.4 (8,17-CH_3), 16.6 (2 × CH_2CH_3), 20.2 (7,18-CH_2), 31.5 ($C(CH_3)_3$), 41.0 ($C(CH_3)_3$), 112.3 (5,20-C), 114.6 (10,15-C), 120.3 (21-C), 129.8, 137.7, 140.0, 140.2 (2^1,3^1-C), 141.0, 142.9 (2^2,3^2-C), 150.6, 150.8, 154.9, 158.3, 175.9. HRMS (ESI) m/z: calcd for $C_{36}H_{36}N_2Se$ + H, 577.2122; found, 577.2135. Anal. calcd for $C_{36}H_{37}N_2Se$; C, 75.11; H, 6.30; N, 4.87. Found: C, 75.52; H, 6.29; N, 4.71.

7,18-Diethyl-8,17-dimethyl-2^3-phenyl-23-selenaazuliporphyrin (9c)

Using the same procedure, tripyrrane analogue **4c** (114 mg, 0.176 mmol) gave the selenaazuliporphyrin (57.1 mg, 0.0958 mmol, 54%) as dark green crystals (chloroform–hexanes). Mp: >300 °C. UV-vis (1% Et_3N–$CHCl_3$): λ_{max} (log ε) 366 (4.66), 402 (4.62), 450 (4.57), 478 (4.60), 621 (4.11), 667 (sh, 4.08). UV-vis (1% TFA–$CHCl_3$): λ_{max} (log ε) 362 (4.57), 398 (sh, 4.52), 508 (4.83), 629 (sh, 4.04), 675 (4.08), 763 (3.64). ^{1}H NMR (500 MHz, $CDCl_3$): δ 1.61 (6H, t, J = 7.7 Hz, 2 × CH_2CH_3), 2.86 (6H, s, 8,17-CH_3), 2.91 (1H, br s, 21-H), 3.42 (4H, q, J = 7.7 Hz, 7,18-CH_2), 7.53 (1H, t, J = 7.4 Hz, *p*-H), 7.63 (2H, t, J = 7.4 Hz, *m*-H), 7.81 (2H, d, J = 7.4 Hz, *o*-H), 8.03 (2H, d, J = 10.4 Hz, 2^2,3^2-H), 8.94 (2H, s, 12,13-H), 9.176 (2H, s, 10,15-H), 9.185 (2H, s, 5,20-H), 9.48 (2H, d, J = 10.4 Hz, 2^1,3^1-H). ^{1}H NMR (500 MHz, acetone-d_6): δ 1.60 (6H, t, J = 7.6 Hz), 2.89 (6H, s), 3.52 (4H, q, J = 7.6 Hz), 7.62 (1H, t, J = 7.4 Hz), 7.69 (2H, t, J = 7.4 Hz), 8.01 (2H, d, J = 7.5 Hz), 8.32 (2H, d, J = 10.6 Hz), 9.08 (2H, s), 9.33 (2H, s), 9.55 (2H, s), 10.00 (2H, d, J = 10.4 Hz). ^{1}H NMR (500 MHz, DMSO-d_6): δ 1.58 (6H, t, J = 7.6 Hz), 2.90 (6H, s), 3.55 (4H, q, J = 7.6 Hz), 7.64 (1H, t, J = 7.4 Hz), 7.71 (2H, t, J = 7.4 Hz), 8.02–8.04 (2H, m), 8.39 (2H, d, J = 10.7 Hz), 9.21 (2H, s), 9.48 (2H, s), 9.64 (2H, s), 10.15 (2H, d, J = 10.7 Hz). ^{1}H NMR (500 MHz, TFA–$CDCl_3$): δ −2.69 (1H, s, 21-H), −1.56 (2H, br s, 2 × NH), 1.80 (6H, t, J = 7.7 Hz, 2 × CH_2CH_3), 3.49 (6H, s, 8,17-CH_3), 4.07 (4H, q, J = 7.7 Hz, 7,18-CH_2), 7.75–7.78 (3H, m, *m*- & *p*-H), 7.94–7.97 (2H, m, *o*-H), 9.07 (2H, d, J = 10.5 Hz, 2^2,3^2-H), 9.92 (2H, s, 12,13-H), 10.32 (2H, d, J = 10.5 Hz, 2^1,3^1-H), 10.72 (2H, s, 10,15-H), 10.83 (2H, s, 5,20-H). ^{13}C NMR ($CDCl_3$): δ 10.8, 17.3, 19.5, 112.0, 115.3, 126.5, 128.5, 129.4, 129.5, 132.8, 133.7, 134.5, 134.6, 137.3, 147.6, 151.5, 156.0. ^{13}C NMR (TFA–$CDCl_3$): δ 11.3 (8,17-CH_3), 16.5 (2 × CH_2CH_3), 20.3 (7,18-CH_2), 112.6 (5,20-C), 114.9 (10,15-C), 119.9 (21-C), 129.3 (*o*-C), 129.9, 130.6 (*p*-C), 132.4 (*m*-C), 138.1, 140.1, 140.5 (2^1,3^1-C), 140.6, 141.4 (12,13-C), 144.1 (2^2,3^2-C), 151.0, 151.3, 154.4, 158.3, 163.4. HRMS (ESI) m/z: calcd for $C_{38}H_{32}N_2Se$ + H, 597.1809; found, 597.1812. Anal. calcd for $C_{38}H_{32}N_2Se$: C, 76.62; H, 5.41; N, 4.70. Found: C, 76.40; H, 5.33; N, 4.67.

2^2-*tert*-Butyl-7,18-diethyl-8,17-dimethyl-21-carba-23-thiabenzo-[*b*]porphyrin (15a)

Potassium hydroxide (240 mg) in methanol (30 mL) was added to a solution of *tert*-butylthiaazuliporphyrin **8b** (21.0 mg, 0.040 mmol) in dichloromethane (30 mL), and the resulting stirred mixture was purged with nitrogen for 10 min. A solution of *tert*-butyl hydroperoxide in decane (5 M, 20 μL) was added, and the resulting solution stirred under nitrogen in the dark at room temperature for 5 h. The solution was diluted with chloroform, washed with water (×2), dried over sodium sulfate, and evaporated under reduced pressure. The residues were chromatographed on a grade 3 alumina column, eluting with 50% dichloromethane–hexanes. The major orange band

was collected, the solvent evaporated, and the residue recrystallized from chloroform–hexanes to give gold-brown crystals (9.0 mg, 0.017 mmol, 43%) corresponding to **15a**. Mp: 263–264 °C, dec. UV-vis (1% Et_3N–$CHCl_3$): λ_{max} (log ε) 390 (4.66), 392 (4.04), 435 (4.85), 529 (4.11), 557 (sh, 4.11), 625 (3.75), 685 (sh, 3.05). UV-vis (1% TFA–$CHCl_3$): λ_{max} (log ε) 420 (4.87), 470 (sh, 4.53), 502 (sh, 4.16), 620 (4.08), 673 (3.52). ^{1}H NMR (50 °C, 500 MHz, $CDCl_3$): δ −5.47 (1H, s, 21-H), −4.41 (1H, br s, NH), 1.76 (9H, s, *t*-Bu), 1.82 (3H, t, J = 7.7 Hz), 1.85 (3H, t, J = 7.7 Hz) (2 × CH_2CH_3), 3.40 (3H, s, 8-CH_3), 3.42 (3H, s, 17-CH_3), 3.92 (2H, q, J = 7.7 Hz, 7-CH_3), 3.96 (2H, q, J = 7.7 Hz, 18-CH_2), 7.81 (1H, dd, J = 7.8, 1.4 Hz, 3^2-H), 8.76 (1H, d, J = 7.8 Hz, 3^1-H), 8.88 (1H, br d, J = 1.4 Hz, 2^1-H), 9.79 (2H, s, 12,13-H), 10.12 (1H, s, 5-H), 10.16 (1H, s, 20-H), 10.300 (1H, s), 10.304 (1H, s) (10,15-H). ^{13}C NMR (50 °C, $CDCl_3$): δ 11.29, 11.33, 17.50, 17.51, 19.91, 19.93, 32.2, 35.6, 105.0 (br), 107.3 (br), 117.0, 117.1, 117.6, 120.2, 124.3, 131.44, 131.51, 134.5 (br), 137.8 (br), 140.8 (br), 141.9, 144.2, 150.6. HRMS (ESI) *m*/*z*: calcd for $C_{35}H_{36}N_2S$ + H, 517.2677; found, 517.2673. HRMS (EI) *m*/*z*: calcd for $C_{35}H_{36}N_2S$, 516.2599; found, 516.2607.

2^2-*tert*-Butyl-7,18-diethyl-8,17-dimethyl-21-carba-23-selenabenzo[*b*]porphyrin (15c)

Potassium hydroxide (240 mg) in methanol (30 mL) was added to a solution of *tert*-butylselenaazuliporphyrin **9c** (22.0 mg, 0.0382 mmol) in dichloromethane (30 mL), was reacted with KOH (240 mg) in methanol (30 mL) and a solution of *tert*-butyl hydroperoxide in decane (5 M, 20 μL) under the foregoing conditions. Recrystallization from chloroform–hexanes gave the selenacarbaporphyrin (8.8 mg, 0.0156 mmol, 41%) as gold-brown crystals. Mp: 275–276 °C, dec. UV-vis (1% Et_3N–$CHCl_3$): λ_{max} (log ε) 400 (sh, 4.58), 444 (4.88), 473 (4.62), 532 (4.02), 567 (3.98), 595 (3.95), 628 (3.89). UV-vis (1% TFA–$CHCl_3$): λ_{max} (log ε) 311 (4.32), 336 (4.34), 440 (4.88), 480 (sh, 4.63), 514 (sh, 4.24), 637 (4.13). ^{1}H NMR (50 °C, 500 MHz, $CDCl_3$): δ −5.35 (1H, s, 21-H), −4.65 (1H, s, NH), 1.77 (9H, s, *t*-Bu), 1.79 (3H, t, J = 7.7 Hz), 1.82 (3H, t, J = 7.7 Hz) (2 × CH_2CH_3), 3.36 (3H, s, 8-CH_3), 3.38 (3H, s, 17-CH_3), 3.87 (2H, q, J = 7.7 Hz, 7-CH_2), 3.92 (2H, q, J = 7.7 Hz, 18-CH_2), 7.81 (1H, dd, J = 7.8, 1.3 Hz, 3^2-H), 8.73 (1H, d, J = 7.8 Hz, 3^1-H), 8.86 (1H, br d, J = 1.3 Hz, 2^1-H), 9.90 (2H, s, 12,13-H), 10.11 (1H, s, 5-H), 10.15 (1H, s, 20-H), 10.37 (1H, s), 10.38 (1H, s) (10,15-H). ^{13}C NMR (50 °C, $CDCl_3$): δ 11.27, 11.32, 17.45, 17.47, 19.91, 19.94, 32.3, 35.6, 106.0 (br), 111.1 (br), 116.9, 117.0, 117.6, 120.2, 124.3, 133.43, 133.48, 136.5 (br), 136.7 (br), 141.6, 143.9, 150.5. HRMS (ESI) *m*/*z*: calcd for $C_{35}H_{36}N_2Se$ + H, 565.2122; found, 565.2123. HRMS (EI) *m*/*z*: calcd for $C_{35}H_{36}N_2Se$, 564.2044; found, 564.2056.

Oxidative ring contraction of 7,18-diethyl-8,17-dimethyl-2^3-phenyl-23-thiaazuliporphyrin (8c)

Potassium hydroxide (240 mg) in methanol (30 mL) was added to a solution of phenylthiaazuliporphyrin **8c** (21.0 mg, 0.0383 mmol) in dichloromethane (30 mL), and the stirred mixture was purged with nitrogen for 10 min. A solution of *tert*-butyl hydroperoxide in decane (5 M, 20 μL) was added, and the resulting solution stirred under nitrogen in the dark at room temperature for 5 h. The solution was diluted with chloroform, washed with water (×2), dried over sodium sulfate, and evaporated under reduced pressure. The residues were chromatographed on a grade 3 alumina column, eluting with 50% dichloromethane–hexanes. The major orange band was collected, the solvent was evaporated, and the residue recrystallized from chloroform–hexanes to give 21-carba-23-thiabenzo[*b*]porphyrin **15b** (7.1 mg, 0.0132 mmol, 34%) as gold-brown crystals, mp: 235 °C, dec. A second minor band was collected (5.2 mg; 0.0092 mmol; 24%) corresponding to the related aldehyde **16b**, mp: 265–266 °C, dec.

7,18-Diethyl-8,17-dimethyl-2^2-phenyl-21-carba-23-thiabenzo[*b*]-porphyrin (15b)

UV-vis (1% Et_3N–$CHCl_3$): λ_{max} (log ε) 394 (4.58), 437 (4.79), 531 (4.00), 559 (3.84), 626 (3.64), 685 (3.02). UV-vis (1% TFA–$CHCl_3$): λ_{max} (log ε) 424 (4.82), 473 (sh, 4.42), 506 (sh, 4.03), 620 (3.97), 675 (3.42). ^{1}H NMR (50 °C, 500 MHz, $CDCl_3$): δ −5.79 (1H, s, 21-H), −4.77 (1H, br s, NH), 1.78–1.81 (6H, 2 overlapping triplets, 2 × CH_2CH_3), 3.373 (3H, s), 3.378 (3H, s) (8,17-CH_3), 3.85–3.91 (4H, 2 overlapping quartets, 7,18-CH_2), 7.51–7.55 (1H, m, *p*-H), 7.68 (2H, t, J = 7.6 Hz, *m*-H), 7.99 (1H, dd, J = 7.6, 1.5 Hz, 3^2-H), 8.08–8.10 (2H, m, *o*-H), 8.86 (1H, d, J = 7.6 Hz, 3^1-H), 9.01 (1H, d, J = 1.5 Hz), 9.75 (2H, s, 12,13-H), 10.06 (1H, s, 5-H), 10.09 (1H, s, 20-H), 10.233 (1H, s), 10.238 (1H, s) (10,15-H). ^{13}C NMR (50 °C, $CDCl_3$): δ 11.3 (2), 17.64, 17.66, 19.82, 19.83, 105.0 (br), 116.8, 119.5, 120.8, 126.2, 127.4, 127.7, 129.2, 131.59, 131.62, 134.4 (br), 136.7 (br), 140.4, 140.7 (br), 142.7, 143.2, 144.6. HRMS (ESI) *m*/*z*: calcd for $C_{37}H_{32}N_2S$ + H, 537.2364; found, 537.2369. HRMS (EI) *m*/*z*: calcd for $C_{37}H_{32}N_2S$, 536.2286; found, 536.2286.

7,18-Diethyl-2^1-formyl-8,17-dimethyl-2^2-phenyl-21-carba-23-thiabenzo[*b*]porphyrin (16b)

UV-vis (1% Et_3N–$CHCl_3$): λ_{max} (log ε) 391 (sh, 4.63), 436 (5.02), 532 (4.18), 562 (4.05), 625 (3.79), 685 (3.55). UV-vis (1% TFA–$CHCl_3$): λ_{max} (log ε) 431 (4.96), 493 (sh, 4.29), 589 (sh, 4.06), 616 (4.11), 670 (3.70). ^{1}H NMR (50 °C, 500 MHz, $CDCl_3$): δ −5.89 (1H, s, 21-H), −4.52 (1H, br s, NH), 1.78 (3H, t, J = 7.6 Hz, 7-CH_2CH_3), 1.85 (3H, t, J = 7.6 Hz, 18-CH_2CH_3), 3.37 (3H, s), 3.38 (3H, s) (8,17-CH_3), 3.87 (2H, q, J = 7.6 Hz, 7-CH_2), 3.93 (2H, q, J = 7.6 Hz, 18-CH_2), 7.55–7.58 (1H, m, *p*-H), 7.64 (2H, t, J = 7.4 Hz, *m*-H), 7.75–7.77 (2H, m, *o*-H), 7.80 (1H, d, J = 7.5 Hz, 3^2-H), 9.04 (1H, d, J = 7.5 Hz, 3^1-H), 9.72–9.76 (2H, AB quartet, J = 4.8 Hz, 12,13-H), 9.99 (1H, s, 5-H), 10.19 (1H, s), 10.25 (1H, s) (10,15-H), 10.71 (1H, s, CHO), 11.34 (1H, s, 20-H). ^{13}C NMR (50 °C, $CDCl_3$): δ 11.24, 11.29, 17.45, 17.50, 19.9, 20.0, 104.7 (br), 107.0 (br), 108.3 (br), 112.2 (br), 118.2, 123.6, 128.1, 128.7, 129.1, 130.8 (br), 131.7, 132.0, 132.4, 133.1 (br), 133.8, 134.0 (br), 136.3 (br), 140.8, 140.9 (br), 141.8 (br), 142.8 (br), 144.9 (br), 141.5, 145.3, 145.6, 196.4. HRMS (ESI) *m*/*z*: calcd for $C_{38}H_{32}N_2OS$ + H, 565.2314; found, 565.2311. HRMS (EI) *m*/*z*: calcd for $C_{38}H_{32}N_2OS$, 564.2235; found, 564.2243.

Oxidative ring contraction 7,18-diethyl-8,17-dimethyl-2^3-phenyl-23-selenaazuliporphyrin (9c)

Phenylselenaazuliporphyrin **9c** (26.0 mg, 0.0436 mmol) was reacted under the foregoing conditions. The crude product was purified by chromatography on grade 3 alumina, eluting with 50% dichloromethane–hexanes. The major orange band was collected, the solvent evaporated, and the residue recrystallized from chloroform–hexanes to give **15d** (9.4 mg, 0.0161 mmol, 37%) as gold-brown crystals, mp: 275–276 °C, dec. A second minor band was collected (5.1 mg, 0.0083 mmol, 19%) corresponding to the related aldehyde **16d**, mp: 179–180 °C, dec.

7,18-Diethyl-8,17-dimethyl-2^2-phenyl-21-carba-23-selenabenzo[*b*]porphyrin (15d)

UV-vis (1% Et_3N–$CHCl_3$): λ_{max} (log ε) 405 (sh, 4.55), 448 (4.89), 474 (4.59), 534 (3.94), 568 (3.98), 595 (3.95), 630 (3.90). UV-vis (1% TFA–$CHCl_3$): λ_{max} (log ε) 440 (4.86), 482 (sh, 4.59), 638 (4.11). ^{1}H NMR (50 °C, 500 MHz, $CDCl_3$): δ −5.65 (1H, s, 21-H), −5.04 (1H, br s, NH), 1.75–1.79 (6H, 2 overlapping triplets, 2 × CH_2CH_3), 3.34 (3H, s), 3.35 (3H, s) (8,17-CH_3), 3.81–3.87 (4H, 2 overlapping quartets, 7,18-CH_2), 7.54 (1H, t, J = 7.4 Hz, *p*-H), 7.70 (2H, t, J = 7.6 Hz, *m*-H) 7.98 (1H, dd, J = 7.6, 1.5 Hz), 8.10 (2H, d, J = 7.6 Hz, *o*-H), 8.81 (1H, d, J = 7.6 Hz, 3^1-H), 8.96 (1H, d, J = 1.5 Hz, 2^1-H), 9.87 (2H, s, 12,13-H), 10.04 (1H, s, 5-H), 10.07 (1H, s, 20-H), 10.31 (1H, s), 10.32 (1H, s) (10,15-H). ^{13}C NMR (50 °C, $CDCl_3$): δ 11.31, 11.33, 17.59, 17.60, 19.8 (2), 106.2 (br), 111.2 (br), 116.7, 119.5, 120.8, 126.1, 127.4, 127.7, 129.2, 133.6, 135.5 (br), 140.3, 142.7, 142.9, 144.3. HRMS (ESI) *m*/*z*: calcd for $C_{37}H_{32}N_2Se$ + H, 585.1809; found, 585.1838. HRMS (EI) *m*/*z*: calcd for $C_{37}H_{32}N_2Se$, 584.1731; found, 584.1750.

7,18-Diethyl-2^1-formyl-8,17-dimethyl-2^2-phenyl-21-carba-23-selenabenzo[*b*]porphyrin (16d)

UV-vis (1% Et_3N–$CHCl_3$): λ_{max} (log ε) 441 (5.02), 474 (4.51), 540 (4.10), 571 (4.05), 629 (3.73), 689 (3.29). UV-vis (1% TFA–$CHCl_3$): λ_{max} (log ε) 311 (4.45), 368 (4.44), 470 (4.96), 509 (4.53), 631 (4.06), 719 (sh, 3.54). ^{1}H NMR (50 °C, 500 MHz, $CDCl_3$): δ −5.50 (1H, s, 21-H), −4.77 (1H, br), 1.78 (3H, t, J = 7.7 Hz, 7-CH_2CH_3), 1.83 (3H, t, J = 7.7 Hz, 18-CH_2CH_3), 3.34 (3H, s, 8-CH_3), 3.36 (3H, s, 17-CH_3), 3.84 (2H, q, J = 7.7 Hz, 7-CH_2), 3.90 (2H, q, J = 7.7 Hz, 18-CH_2), 7.54–7.58 (1H, m, *p*-H), 7.63 (2H, t, J = 7.5 Hz, *m*-H), 7.74–7.77 (2H, m, *o*-H), 7.78 (1H, d, J = 7.6 Hz, 3^2-H), 9.00 (1H, d, J = 7.6 Hz, 3^1-H), 9.87–9.90 (2H, AB quartet, J = 5.5 Hz, 12,13-H), 10.02 (1H, s, 5-H), 10.30 (1H, s, 10-H), 10.35 (1H, s, 15-H), 10.71 (1H, s, CHO, 11.34 (1H, s). ^{13}C NMR (50 °C, $CDCl_3$): δ 11.24, 11.26, 17.3, 17.5, 19.9, 20.0, 111.5 (br), 117.8, 117.9, 123.6, 128.1, 128.7, 129.0, 130.8, 132.2 (br), 132.4, 133.9, 134.0, 135.0 (br), 140.8, 141.0, 145.3, 196.4. HRMS (EI) *m*/*z*: calcd for $C_{38}H_{32}N_2Ose$, 612.1680; found, 612.1689.

2^3-*tert*-Butyl-7,18-tetraethyl-8,17-dimethyl-23-oxaazuliporphyrin dihydrochloride (12b·2HCl)

Azulitripyrrane analogue **4b** (115 mg, 0.183 mmol) was stirred in TFA (3 mL) under nitrogen for 10 min. The reaction mixture was diluted with dichloromethane (100 mL), 2,5-furandicarboxaldehyde (23 mg; 0.18 mmol) was added, and the reaction mixture stirred overnight in the dark. The solution was shaken vigorously in a separatory funnel with 0.1% aqueous ferric chloride solution (150 mL) for 5 min. The organic layer was separated and then shaken with a saturated aqueous sodium chloride solution. A precipitate formed that was collected by suction filtration and this was dissolved in methanol and evaporated under reduced pressure. The residue was purified by chromatography on a silica gel column eluting with 10–15% methanol–chloroform. A bright green fraction was collected and 2 mL of a 1 M solution of hydrogen chloride in diethyl ether was added. Following evaporation of the solvent, the residue was dissolved in hot 10% ethanol–chloroform and brought to a saturation point with hexanes. Upon cooling, a dark green solid was collected by suction filtration and following drying *in vacuo* the oxaazuliporphyrin hydrochloride salt (60.4 mg, 0.103 mmol, 57%) was obtained as a dark green solid. Mp: >300 °C. UV-vis (1% MeOH–$CHCl_3$): λ_{max} (log ε) 348 (4.54), 377 (4.55), 464 (4.91), 594 (sh, 3.81), 645 (4.24), 725 (sh, 3.58). UV-vis (TFA (1%)–MeOH (1%)–$CHCl_3$): λ_{max} (log ε) 355 (4.57), 372 (4.56), 461 (4.92), 593 (sh, 3.78), 647 (4.24), 723 (sh, 3.55). UV-vis (DBU (2%)–MeOH (1%)–$CHCl_3$): λ_{max} (log ε) 362 (4.64), 432 (4.68), 452 (sh, 4.59), 476 (sh, 4.40), 525 (sh, 3.99), 560 (3.89), 627 (3.90), 685 (3.91). ^{1}H NMR (500 MHz, CD_3OD): δ −3.78 (1H, s, 21-H), 1.80 (9H, br s, *t*-Bu), 1.85 (6H, br, 2 × CH_2CH_3), 3.57 (6H, s, 8,17-CH_3), 4.22 (4H, br, 7,18-CH_2), 9.20 (2H, br, 2^2,3^2-H), 10.13 (2H, s, 12,13-H), 10.42 (2H, s, 10,15-H), 10.56 (2H, br, 2^1,3^1-H), 11.11 (2H, br s, 5,20-H). ^{1}H NMR (500 MHz, TFA–$CDCl_3$): δ −3.55 (1H, s, 21-H), 1.74 (9H, s, *t*-Bu), 1.78 (6H, br, 2 × CH_2CH_3), 3.45 (6H, s, 8,17-CH_3), 4.04 (4H, br, 7,18-CH_2), 8.96 (2H, br, 2^2,3^2-H), 9.76 (2H, s, 12,13-H), 9.89 (2H, s, 10,15-H), 10.09 (2H, br, 2^1,3^1-H), 10.66 (2H, br s, 5,20-H). ^{1}H NMR (500 MHz, DBU–$CDCl_3$, downfield region only): δ 7.91 (2H, d, J = 10.6 Hz), 8.17 (2H, s), 8.45 (2H, s), 9.02 (2H, s), 9.27 (2H, d, J = 10.6 Hz). ^{13}C NMR (CD_3OD): δ 11.4 (8,17-CH_3), 17.4 (2 × CH_2CH_3), 20.9 (7,18-CH_2), 32.0 ($C(CH_3)_3$), 41.6 ($C(CH_3)_3$), 98.0 (10,15-C), 113.9 (5,20-C), 125.9 (21-C), 131.7, 135.0 (12,13-C), 137.5, 141.6, 142.6 (2^1,3^1-C), 144.5 (2^2,3^2-C), 145.5, 149.9, 154.8, 159.0, 176.3. ^{13}C NMR (TFA–$CDCl_3$): δ 11.3 (8,17-CH_3), 17.0 (2 × CH_2CH_3), 20.4 (7,18-CH_2), 31.7 ($C(CH_3)_3$), 40.9 ($C(CH_3)_3$), 96.8 (10,15-C), 112.3 (5,20-C), 126.3 (21-C), 130.0, 133.5 (12,13-C), 136.2, 140.3 (2^1,3^1-C), 140.7, 142.7 (2^2,3^2-C), 144.9, 148.9, 153.6, 157.3, 175.0. HRMS (ESI) *m*/*z*: calcd for $C_{36}H_{36}N_2O$ + H, 513.2906; found, 513.2913.

7,18-Tetraethyl-8,17-dimethyl-23-oxaazuliporphyrin dihydrochloride (12a·2HCl)

Azulitripyrrane **4a** (103 mg, 0.18 mmol) was reacted with 2,5-furandicarbaldehyde (23 mg, 0.18 mmol) under the foregoing conditions and gave oxaazuliporphyrin dihydrochloride

12a·2HCl (51.1 mg, 0.096 mmol, 53%) as a dark solid. Mp: >300 °C; UV-vis (1% MeOH–$CHCl_3$): λ_{max} (log ε) 348 (4.62), 386 (4.57), 436 (sh, 4.59), 467 (4.94), 496 (sh, 4.57), 597 (sh, 3.88), 648 (4.30), 737 (sh, 3.61). UV-vis (TFA (1%)–MeOH (1%)–$CHCl_3$): λ_{max} (log ε) 348 (4.66), 385 (4.59), 434 (sh, 4.64), 462 (4.99), 597 (sh, 3.87), 650 (4.34). UV-vis (DBU (2%)–MeOH (1%)–$CHCl_3$): λ_{max} (log ε) 366 (4.58), 441 (4.81), 525 (4.05), 562 (4.01), 626 (3.88), 687 (3.78). ^{1}H NMR (500 MHz, CD_3OD): δ −3.49 (1H, s, 21-H), 1.81 (6H, t, J = 7.7 Hz, 2 × CH_2CH_3), 3.53 (6H, s, 8,17-CH_3), 4.17 (4H, q, J = 7.7 Hz, 7,18-CH_2), 8.85 (1H, br t, J = 9.0 Hz, 2^3-H), 8.95 (2H, br, 2^2,3^2-H), 10.09 (2H, br s, 12,13-H), 10.35 (2H, br s, 10,15-H), 10.62 (2H, d, J = 9.2 Hz, 2^1,3^1-H), 11.05 (2H, br s, 5,20-H). ^{1}H NMR (500 MHz, TFA–$CDCl_3$): δ −3.21 (1H, s, 21-H), −0.50 (2H, br s, 2 × NH), 1.77 (6H, t, J = 7.3 Hz, 2 × CH_2CH_3), 3.45 (6H, s, 8,17-CH_3), 4.04 (4H, q, J = 7.3 Hz, 7,18-CH_2), 8.67 (1H, br t, J = 9.2 Hz, 2^3-H), 8.78 (2H, br t, J = 8.5 Hz, 2^2,3^2-H), 9.78 (2H, s, 12,13-H), 9.90 (2H, s, 10,15-H), 10.14 (2H, br d, J = 8.3 Hz, 2^1,3^1-H), 10.66 (2H, s, 5,20-H). ^{1}H NMR (500 MHz, DBU–$CDCl_3$, downfield region only): δ 7.61 (2H, t, J = 9.6 Hz), 7.69 (1H, t, J = 9.5 Hz), 8.03 (2H, s), 8.35 (2H, s), 8.90 (2H, s), 9.20 (2H, d, J = 9.5 Hz). ^{13}C NMR (50 °C, CD_3OD): δ 11.1 (8,17-CH_3), 17.1 (2 × CH_2CH_3), 20.6 (7,18-CH_2), 97.9 (10,15-C), 113.9 (5,20-C), 126.5 (21-C), 131.3, 135.0 (12,13-C), 137.5, 141.8, 143.5 (2^1,3^1-C), 145.8 (2^2,3^2-C), 146.3, 149.3 (2^3-C), 150.2, 156.1, 159.3. ^{13}C NMR (TFA–$CDCl_3$): δ 11.1 (8,17-CH_3), 16.7 (2 × CH_2CH_3), 20.2 (7,18-CH_2), 97.0 (10,15-C), 112.2 (5,20-C), 126.4 (21-C), 129.6, 133.9 (12,13-C), 136.6, 140.8, 141.3 (2^1,3^1-C), 144.2 (2^2,3^2-C), 145.6, 147.6 (2^3-C), 149.6.2, 154.8, 157.9. HRMS (ESI) m/z: calcd for $C_{32}H_{28}N_2O$ + H, 457.2280; found, 457.2279.

7,18-Tetraethyl-8,17-dimethyl-2^3-phenyl-23-oxaazuliporphyrin dihydrochloride (12c·2HCl)

Using the previous procedure, azulitripyrrane **4c** (116.5 mg, 0.18 mmol) was reacted with 2,5-furandicarbaldehyde (23 mg, 0.18 mmol) to give oxaazuliporphyrin dihydrochloride **12c**·2HCl (45.1 mg, 0.074 mmol, 41%) as a dark solid. Mp: >300 °C. UV-vis (1% MeOH–$CHCl_3$): λ_{max} (log ε) 348 (4.65), 386 (4.61), 467 (4.97), 495 (sh, 4.61), 597 (sh, 3.93), 648 (4.35), 734 (sh, 3.62). UV-vis (TFA (1%)–MeOH (1%)–$CHCl_3$): λ_{max} (log ε) 348 (4.68), 385 (4.62), 463 (5.02), 492 (sh, 4.62), 598 (sh, 3.90), 650 (4.37). UV-vis (DBU (2%)–MeOH (1%)–$CHCl_3$): λ_{max} (log ε) 365 (4.65), 443 (4.84), 524 (4.10), 563 (4.09), 626 (3.98), 686 (3.90). ^{1}H NMR (500 MHz, 50 °C, CD_3OD): δ −3.57 (1H, s, 21-H), 1.82 (6H, t, J = 7.7 Hz, 2 × CH_2CH_3), 3.55 (6H, s, 8,17-CH_3), 4.19 (4H, q, J = 7.7 Hz, 7,18-CH_2), 7.72–7.78 (3H, m, m- and p-H), 8.09–8.12 (2H, m, o-H), 9.14 (2H, br, 2^2,3^2-H), 10.11 (2H, s, 12,13-H), 10.39 (2H, s, 10,15-H), 10.58 (2H, br d, J = 10.1 Hz, 2^1,3^1-H), 11.08 (2H, br s, 5,20-H). ^{1}H NMR (500 MHz, TFA–$CDCl_3$): δ −3.39 (1H, s, 21-H), −0.84 (2H, br, 2 × NH), 1.80 (6H, br, 2 × CH_2CH_3), 3.49 (6H, s, 8,17-CH_3), 4.08 (4H, br, 7,18-CH_2), 7.76 (3H, br, m- and p-H), 7.93 (2H, br, o-H), 8.98 (2H, br, 2^2,3^2-H), 9.82 (2H, br s, 12,13-H), 9.96 (2H, br s, 10,15-H), 10.14 (2H, br, 2^1,3^1-H), 10.70 (2H, br s, 5,20-H). ^{13}C NMR (CD_3OD): δ 11.2 (8,17-CH_3), 17.1 (2 × CH_2CH_3), 20.6 (7,18-CH_2), 97.9 (10,15-C), 113.9 (5,20-C), 125.9 (21-H), 130.3 (o-C), 131.0 (m-C), 132.4 (p-C), 135.1 (12,13-C), 137.5, 141.7, 142.5 (2^1,3^1-C), 145.1 (2^2,3^2-C), 146.0, 150.1, 154.4, 159.3. ^{13}C NMR (TFA–$CDCl_3$): δ 11.2 (8,17-CH_3), 16.8 (2 × CH_2CH_3), 20.3 (7,18-CH_2), 97.0 (10,15-C), 112.2 (5,20-C), 125.4 (21-H), 129.2 (o-C), 130.2, 130.6 (m-C), 132.2 (p-C), 133.9 (12,13-C), 136.8, 140.3 (2^1,3^1-C), 140.8, 143.9 (2^2,3^2-C), 145.4, 149.6, 152.9, 157.9, 162.9. HRMS (ESI) m/z: calcd for $C_{38}H_{32}N_2O$ + H, 533.2593; found, 533.2590.

Crystallographic experimental details of 8b·$CHCl_3$

X-ray quality crystals of **8b·$CHCl_3$** were suspended in oil at ambient temperature and a suitable crystal was selected. A black prism thereby obtained of approximate dimensions 0.59 mm × 0.18 mm × 0.09 mm was mounted and transferred to a Bruker PLATFORM diffractometer equipped with a SMART 1000 CCD area detector. The X-ray diffraction data were collected at −80 °C using Mo-K_α (λ = 0.71073 Å) radiation. Data collection and cell refinement were performed using SMART and SAINT, respectively.[25] The unit cell parameters were obtained from a least-squares refinement of 5399 centered reflections. Compound **8b·$CHCl_3$** was found to crystallize in the orthorhombic crystal system with the following unit cell parameters: a = 23.252(3) Å, b = 8.8725(10) Å, c = 16.3422(18) Å, Z = 4. The crystal system and systematic absences indicated the space group to be $Pna2_1$ (no. 33) or $Pnam$ (no. 62).[26] The former was chosen on the basic that E-statistics strongly suggested a noncentrosymmetric structure and a sensible, quality refinement was obtained. A total of 24 851 reflections were collected, of which 6878 were unique, and 4888 were observed $F_o^2 > 2\sigma(F_o^2)$. Limiting indices were as follows: $-28 \leq h \leq 28$, $-11 \leq k \leq 11$, $-20 \leq l \leq 20$. Data reduction were accomplished using SAINT.[25] The data were corrected for absorption using the SADABS procedure.[25] Solution and data analysis were performed using the WinGX software package.[27] The structure of **8b·$CHCl_3$** was solved by direct methods using the program SIR2004[28] and the refinement was completed using the program SHELX2013.[29,30] All non-hydrogen atoms were refined anisotropically. The H atoms attached to atom C21 was identified through difference Fourier synthesis and refined with isotropic displacement parameters. All other H atoms were included in the refinement in the riding-model approximation (C–H Ar, CH_3, CH_2, CH = 0.95, 0.98, 0.99, and 1.00 Å), with isotropic displacement parameters fixed at Ar, CH_2, CH = 1.2$U_{eq.}$ and CH_3 = 1.5$U_{eq.}$ of the parent atom. The *tert*-butyl group was rotationally disordered and required use of SAME and EADP instructions in SHELXL2013 to achieve a sensible refinement. Full-matrix least-squares refinement on F^2 led to convergence, $(\Delta/\sigma)_{max}$ = 0.000, $(\Delta/\sigma)_{mean}$ = 0.0000, with R_1 = 0.0537 and wR_2 = 0.1317 for 6878 data with $F_o^2 > 2\sigma(F_o^2)$ using 7 restraints and 392 parameters. A final difference Fourier synthesis showed features in the range of $\Delta\rho_{max}$ = 0.349 e$^-$ Å^{-3} to $\Delta\rho_{min}$ = −0.319 e$^-$ Å^{-3} which were deemed of no chemical significance. Molecular diagrams were generated using ORTEP-3[27] and POV-Ray.[31] CCDC 958530 contains the supplementary crystallographic data for this structure.

Crystallographic experimental details of 9b·CHCl$_3$

X-ray quality crystals of **9b·CHCl$_3$** were suspended in oil at ambient temperature and a suitable crystal was selected. A black prism thereby obtained of approximate dimensions 0.55 mm × 0.14 mm × 0.07 mm was mounted and transferred to a Bruker PLATFORM diffractometer equipped with a SMART 1000 CCD area detector. The X-ray diffraction data were collected at −80 °C using Mo-K$_\alpha$ (λ = 0.71073 Å) radiation. Data collection and cell refinement were performed using SMART and SAINT, respectively.[25] The unit cell parameters were obtained from a least-squares refinement of 4421 centered reflections. Compound **9b·CHCl$_3$** was found to crystallize in the monoclinic crystal system with the following unit cell parameters: a = 8.1545(7) Å, b = 26.714(2) Å, c = 15.641(1) Å, β = 104.854(1)°, Z = 4. The crystal system and systematic absences indicated the space group to be $P2_1/n$ (no. 14).[26] A total of 25 729 reflections were collected, of which 6742 were unique, and 5219 were observed $F_o^2 > 2\sigma(F_o^2)$. Limiting indices were as follows: $-10 \le h \le 10$, $-33 \le k \le 33$, $-19 \le l \le 19$. Data reduction were accomplished using SAINT.[25] The data were corrected for absorption using the SADABS procedure.[25] Solution and data analysis were performed using the WinGX software package.[27] The structure of **9b·CHCl$_3$** was solved by direct methods using the program SIR2004[28] and the refinement was completed using the program SHELX2013.[29,30] All non-hydrogen atoms were refined anisotropically. The H atoms attached to atom C21 was identified through difference Fourier synthesis and refined with isotropic displacement parameters. All other H atoms were included in the refinement in the riding-model approximation (C–H Ar, CH_3, CH_2, CH = 0.95, 0.98, 0.99, and 1.00 Å), with isotropic displacement parameters fixed at Ar, CH_2, CH = 1.2$U_{eq.}$ and CH_3 = 1.5$U_{eq.}$ of the parent atom. Full-matrix least-squares refinement on F^2 led to convergence, $(\Delta/\sigma)_{max}$ = 0.000, $(\Delta/\sigma)_{mean}$ = 0.0000, with R_1 = 0.0438 and wR_2 = 0.1089 for 5219 data with $F_o^2 > 2\sigma(F_o^2)$ using 0 restraints and 394 parameters. A final difference Fourier synthesis showed features in the range of $\Delta\rho_{max}$ = 1.104 e$^-$ Å^{-3} to $\Delta\rho_{min}$ = −1.000 e$^-$ Å^{-3} which were deemed of no chemical significance. Molecular diagrams were generated using ORTEP-3[27] and POV-Ray.[31] CCDC 958523 contains the supplementary crystallographic data for this structure.

Acknowledgements

This material is based upon work supported by the National Science Foundation under Grant no. CHE-1212691 and CHE-0348158 and the Petroleum Research Fund, administered by the American Chemical Society. We thank Dr Robert McDonald and The University of Alberta Structure Determination Laboratory for collecting the X-ray data.

References

1 T. D. Lash, in *Handbook of Porphyrin Science – With Applications to Chemistry, Physics, Material Science, Engineering, Biology and Medicine*, ed. K. M. Kadish, K. M. Smith and R. Guilard, World Scientific Publishing, Singapore, 2012, vol. 16, pp. 1–329.
2 T. D. Lash, *Eur. J. Org. Chem.*, 2007, 5461–5481.
3 M. Pawlicki and L. Latos-Grazynski, in *Handbook of Porphyrin Science – With Applications to Chemistry, Physics, Material Science, Engineering, Biology and Medicine*, ed. K. M. Kadish, K. M. Smith and R. Guilard, World Scientific Publishing, Singapore, 2010, vol. 2, pp. 103–192.
4 M. Toganoh and H. Furuta, in *Handbook of Porphyrin Science – With Applications to Chemistry, Physics, Material Science, Engineering, Biology and Medicine*, ed. K. M. Kadish, K. M. Smith and R. Guilard, World Scientific Publishing, Singapore, 2010, vol. 2, pp. 103–192.
5 T. D. Lash, *J. Porphyrins Phthalocyanines*, 2011, **15**, 1093–1115.
6 (*a*) H. Furuta, T. Ogama, Y. Uwatoko and K. Araki, *Inorg. Chem.*, 1999, **38**, 2676–2682; (*b*) M. A. Muckey, L. F. Szczepura, G. M. Ferrence and T. D. Lash, *Inorg. Chem.*, 2002, **41**, 4840–4842; (*c*) T. D. Lash, D. A. Colby and L. F. Szczepura, *Inorg. Chem.*, 2004, **43**, 5258–5267.
7 K. B. Fields, J. T. Engle, S. Sripothongnak, C. Kim, X. P. Zhang and C. J. Ziegler, *Chem. Commun.*, 2011, **47**, 749–757.
8 T. D. Lash and S. T. Chaney, *Angew. Chem., Int. Ed. Engl.*, 1997, **36**, 839–840.
9 T. D. Lash, D. A. Colby, S. R. Graham and S. T. Chaney, *J. Org. Chem.*, 2004, **69**, 8851–8864.
10 S. R. Graham, D. A. Colby and T. D. Lash, *Angew. Chem., Int. Ed.*, 2002, **41**, 1371–1374.
11 T. D. Lash, A. D. Lammer, A. S. Idate, D. A. Colby and K. White, *J. Org. Chem.*, 2012, **77**, 2368–2381.
12 (*a*) D. A. Colby and T. D. Lash, *Chem.–Eur. J.*, 2002, **8**, 5397–5402; (*b*) T. D. Lash, D. A. Colby and G. M. Ferrence, *Eur. J. Org. Chem.*, 2003, 4533–4548.
13 T. D. Lash, J. A. El-Beck and G. M. Ferrence, *J. Org. Chem.*, 2007, **72**, 8402–8415.
14 (*a*) S. R. Graham, G. M. Ferrence and T. D. Lash, *Chem. Commun.*, 2002, 894–895; (*b*) T. D. Lash, D. A. Colby, S. R. Graham, G. M. Ferrence and L. F. Szczepura, *Inorg. Chem.*, 2003, **42**, 7326–7338.
15 T. D. Lash, K. Pokharel, M. Zeller and G. M. Ferrence, *Chem. Commun.*, 2012, **48**, 11793–11795.
16 T. D. Lash, *Chem. Commun.*, 1998, 1683–1684.
17 D. A. Colby, G. M. Ferrence and T. D. Lash, *Angew. Chem., Int. Ed.*, 2004, **43**, 1346–1349.
18 T. Okujima, T. Kikkawa, H. Nakano, H. Kubota, N. Fukugami, N. Ono, H. Yamada and H. Uno, *Chem.–Eur. J.*, 2012, **18**, 12854–12863.
19 S. Venkatraman, V. G. Anand, V. PrabhuRaja, H. Rath, J. Sankar, T. K. Chandrashekar, W. Teng and K. R. Senge, *Chem. Commun.*, 2002, 1660–1661.
20 Z. Zhang, G. M. Ferrence and T. D. Lash, *Org. Lett.*, 2009, **11**, 101–104.
21 J. A. El-Beck and T. D. Lash, *Eur. J. Org. Chem.*, 2007, 3981–3990.

22 J.-i. Aihara, *J. Phys. Chem. A*, 2008, **112**, 5305–5311.
23 A. Ghosh, T. Wondimagegn and H. J. Nilsen, *J. Phys. Chem. B*, 1998, **102**, 10459–10467.
24 T. D. Lash, *J. Porphyrins Phthalocyanines*, 2012, **16**, 423–433.
25 (*a*) Bruker, *SMART CCD software package, version 5.630*, Bruker Advanced X-ray Solutions, Madison, Wisconsin, 1997–2002; (*b*) Bruker, *SAINT+ Integration Software for Single Crystal Data frames - h,k,l, intensity, version 6.45*, Bruker Advanced X-ray Solutions, Madison, Wisconsin, 2003; (*c*) Bruker, *SADABS-Empirical absorption correction procedures*, Bruker Advanced X-ray Solutions, Madison, Wisconsin, 2003.
26 P. McArdle, *J. Appl. Crystallogr.*, 1996, **29**, 306.
27 L. J. Farrugia, *J. Appl. Crystallogr.*, 2012, **45**, 849–854.
28 M. C. Burla, R. Caliandro, M. Camalli, B. Carrozzini, G. L. Cascarano, L. De Caro, C. Giacovazzo, G. Polidori and R. Spagna, *J. Appl. Crystallogr.*, 2005, **38**, 381–388.
29 G. M. Sheldrick, *Acta Crystallogr., Sect. A: Fundam. Crystallogr.*, 2008, **64**, 112–122.
30 G. M. Sheldrick, *SHELX2013*, University of Göttingen, Germany, 2013.
31 Persistence of Vision Team, 2006, http://www.povray.org